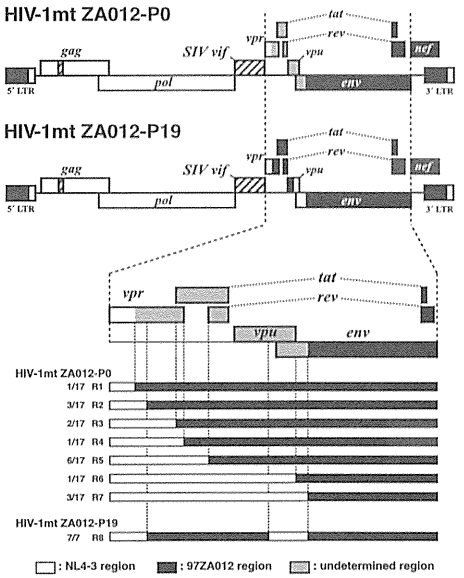

Fig. 4. Recombination breakpoints in HIV-1mt ZA012-P0 and ZA012-P19 genomes. The genome organizations of HIV-1mt ZA012-P0 and HIV-1mt ZA012-P19 are schematically represented (upper two diagrams). The region from the initiation of *vpr* to the end of *env* that included recombination breakpoint sites is depicted in the third diagram; the HIV-1mt ZA012-P0 (17 SGA sequences) or HIV-1mt ZA012-P19 (seven SGA sequences) are depicted (bottom). Sequences from HIV-1mt ZA012-P0 were classified into seven patterns of recombination breakpoints (R1 to R7). Sequences from HIV-1mt ZA012-P19 were classified into one recombination breakpoint pattern (R8). The numbers (left) indicate the numbers of sequences per analyzed sequence.

breakpoints in the region (Fig. 4). One recombination breakpoint was detected at nucleotide positions 178–187 of the *vpr* gene in 1/17 SGA sequences (5736–5745 in HXB2 numbering, recombination type R1) with 10 identical base pairs between NL-DT5R and 97ZA012. In addition to R1, we identified the following recombination types: the *vpr* gene in 3/17 SGA sequences (5760–5767; R2), the initiation of *tat* in 2/17 SGA sequences, (5821–5839; R3), the end of the *vpr* gene in 1/17 SGA sequence (5852–5865; R4), the initiation of *rev* in 6/17 SGA sequences (5960–6000; R5), the end of the *vpu* gene in 1/17 SGA sequence (6357–6392; R6) and the upstream of V1/V2 of the *env* gene in 3/17 SGA sequences (6467–6491; R7). These results suggest that homologous recombination occurs in various sites with homologous sequences.

Next, seven SGA sequences were amplified from viral RNA isolated from the culture supernatant of PtM PBMCs infected with HIV-1mt ZA012-P19, and nucleotide sequences and recombination breakpoints were determined in the same manner. Unexpectedly, all the sequences of HIV-1mt ZA012-P19 had three recombination breakpoints in the region from the *vpr* to *env* genes (recombination type R8 in Fig. 4). The first breakpoint was located in the *vpr* gene (5760–5767), the second was located in the *vpu* gene (6194–6213), and the third was located in *env* (6467–6491) with the N-terminal portion of C1 region from NL4-3 sequence. Although the pattern of recombination breakpoint of the virus differed from those of HIV-1mt ZA012-P0, the first and third recombination breakpoints were identical to the recombination type of R2 and R7, respectively (Fig. 4). It is likely that HIV-1mt ZA012-P19 was generated from further recombination events that occurred in the middle of the *vpu* gene (6194–6213) between recombination type R2 and R7 of HIV-1mt ZA012-P0.

It is conceivable that the genome of HIV-1mt ZA012-P19 acquired several amino acid mutations associated with the enhanced replication in PtM PBMCs. Compared with the deduced amino acid sequences in HIV-1mt ZA012-P0, HIV-1mt ZA012-P19 acquired substitutions from Lys to Arg at amino acid position 432 in Pol-RT and Asp to Glu at position 232 in Pol-IN that were in the NL-DT5R backbone. In addition, an amino acid substitution from Phe to Ser at 139 in Nef was found in HIV-1mt ZA012-P19 compared to 17 SGA sequences derived from HIV-1mt ZA012-P0. No nonsynonymous substitutions were identified in Gag and Vif, the proteins responsible for evading TRIM5α and APOBEC3. Around the recombination break points in HIV-1mt ZA012-P19, the *vpr* and *vpu* genes keep each open reading frame and do not contain any mutations in the region derived from NL-DT5R, respectively. Furthermore, consensus amino acid sequence of HIV-1mt ZA012-P0 and -P19 were also identical in the regions derived from HIV-1 97ZA012, respectively. These facts suggest that recombination was occurred to keep these genes intact.

Phylogenetic analysis of env genes

It is likely that HIV-1mt ZA012-P0 generated by IHR in human C8166-CCR5 cells was a swarm carrying diverse *env* sequences of the parental HIV-1 97ZA012, which evolved to HIV-1mt ZA012-P19 through *in vitro* passages. To evaluate the *env* variants selected in C8166-CCR5 cells or primary PtM cells, we determined 22 sequences of HIV-1 97ZA012, 17 sequences of HIV-1mt ZA012-P0

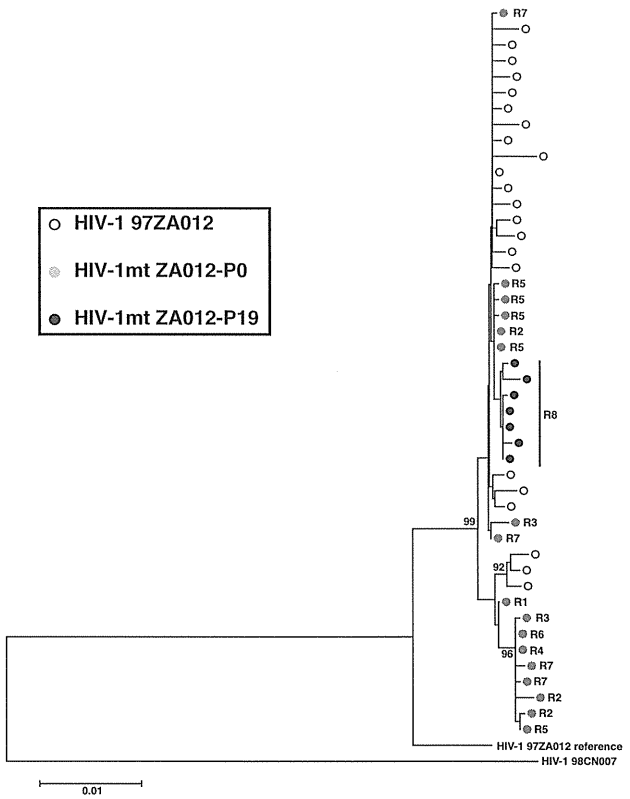

Fig. 5. Phylogenic analysis of partial *env* sequences. A neighbor-joining phylogenic tree was constructed from the partial nucleic acid sequences of *env* (nucleotide positions 211–2571 based on *env* of HXB2 numbering). The sequences of HIV-1 97ZA012 (white circle), HIV-1mt ZA012-P0 (grey circle) and HIV-1mt ZA012-P19 (black circle) were determined from SGA sequences. HIV-1 97ZA012 (accession number: AF286227) and 98CN007 (AF286230) reference sequences were obtained from the Los Alamos HIV sequence database (http://hiv-web.lanl.gov/). R1–R8 correspond to the patterns of recombination breakpoint types in Fig. 2. Bootstrap values were computed from 1000 bootstrap replicates, and only > 90% are shown at branches. The scale bar indicates the substitutions per site.

and seven sequences of HIV-1mt ZA012-P19 from SGA. Next, we conducted a phylogenetic analysis of the nucleotide sequences of the 3′ terminal 2361 bp of each viral *env* derived from HIV-1 97ZA012 and shared by all variants of HIV-1mt ZA012-P0 and -P19 (Fig. 5). These sequences were divided into two clusters: the larger cluster included 19 sequences of HIV-1 97ZA012, 8 sequences of HIV-1mt ZA012-P0 and 7 sequences of HIV-1mt ZA012-P19; and the smaller cluster included 3 sequences of HIV-1 97ZA012 and 9 sequences of HIV-1mt ZA012-P0. Recombination types R2, R3, R5 and R7 (Fig. 4) were intermingled among the sequences of the two groups, suggesting that homologous recombination could occur in various *env* templates.

To compare the genetic diversity of *env* in these viruses, we computed the mean of all pair-wise distances between any two viral *env* sequences in each of the viruses. The computed diversity of *env* in HIV-1mt ZA012-P0 was 0.0038 ± 0.0025 ($\pm$ standard deviation, SD), which was significantly lower than that in the parental HIV-1 97ZA012 (0.0044 ± 0.0021; $p < 0.05$). The computed diversity of HIV-1mt ZA012-P19 *env* was 0.0012 ± 0.00078, which showed significantly lower variation compared to HIV-1mt ZA012-P0 ($p < 0.0001$).

Co-receptor usage of HIV-1mt ZA012-P19

To characterize co-receptor usage of HIV-1mt ZA012-P19 after long-term *in vitro* passage, we conducted an entry assay using TZM-bl cells with small molecule antagonists (Fig. 6). Viral infectivity of the CXCR4-tropic virus (NL4-3) was reduced in the presence of an increasing amount of the CXCR4 inhibitor, AMD3100, but was not affected by the CCR5 inhibitor, AD101. In contrast, the CCR5-tropic virus, SIVmac239, was inhibited in the presence of an increasing amount of AD101 but not by AMD3100. Similar to the results using SIVmac239, HIV-1mt ZA012-P19 exhibited sensitivity to inhibition by AD101 but resistance to AMD3100, indicating that the virus maintained its CCR5-tropism after the serial passage.

Replication of HIV-1mt ZA012 in pig-tailed macaques

Since HIV-1mt ZA012-P19 utilized CCR5 as a co-receptor and exhibited increased infectivity to primary cells of PtMs, we next assessed the *in vivo* replication capacity of the virus by experimental infection of PtMs. Two PtMs were inoculated intravenously

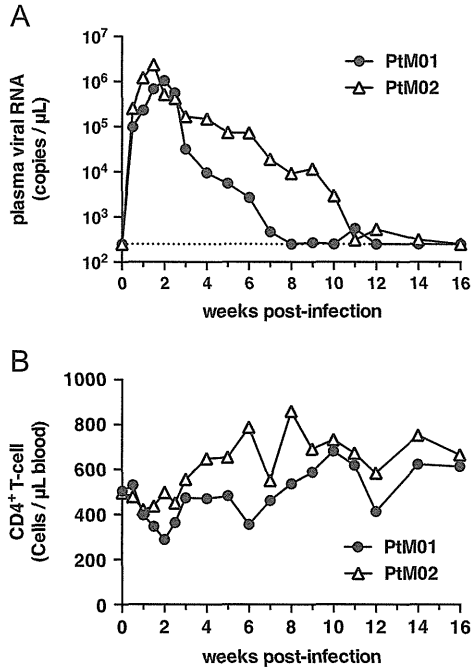

Fig. 7. HIV-1mt ZA012 infection of pig-tailed macaques. Two pig-tailed macaques were inoculated intravenously with HIV-1mt ZA012 (100,000 $TCID_{50}$), and the plasma viral RNA burdens (A) and circulating $CD4^+$ T-lymphocytes (B) were monitored.

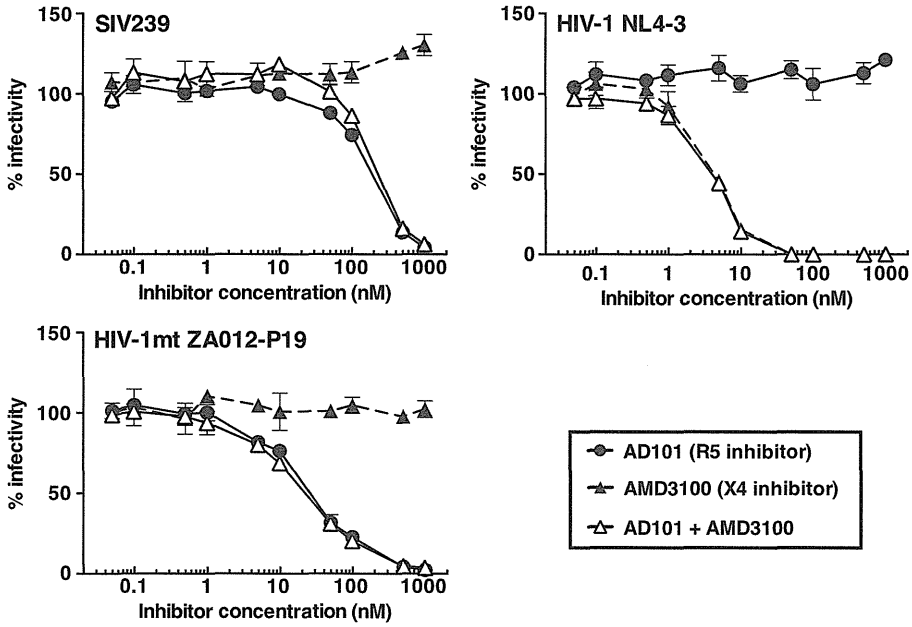

Fig. 6. Co-receptor usage of HIV-1mt ZA012-P19. Infectivity of HIV-1 NL4-3, SIVmac239 and HIV-1mt ZA012-P19 to TZM-bl cells was assessed in the presence of increasing amounts of AMD3100 (CXCR4 inhibitor), AD101 (CCR5 inhibitor) or both. The experiment was conducted in triplicate.

with 1.0×10^5 $TCID_{50}$ of the HIV-1mt prepared in PtM PBMCs, and plasma viral RNA burdens and the numbers of circulating $CD4^+$ T-lymphocytes were monitored periodically (Fig. 7A). Plasma viral RNA loads in PtM01 peaked (1.0×10^6 copies/mL) at 2 weeks post-infection (wpi) and declined thereafter to levels below the detection limit at 8 wpi. PtM02 exhibited a peak plasma viral RNA burden (2.3×10^6 copies/mL) at 1.5 wpi and maintained more than 1×10^4 copies/mL by 9 wpi, but the viral load declined to levels below the detection limit at 16 wpi. The numbers of $CD4^+$ T-lymphocytes in the circulation in both animals were not affected (Fig. 7B). Furthermore, we analyzed naive and memory populations of $CD4^+$ T cells and no preferential depletion of circulating memory $CD4^+$ T-lymphocyte was observed (data not shown).

Discussion

In this study, we used IHR to generate a new HIV-1mt carrying *env* from the CCR5-tropic subtype C HIV-1 clinical isolate. This recombination method has been used to generate infectious HIV-1 or SHIV by joining two linear DNAs in regions with completely identical sequences (Chen et al., 2000; Kalyanaraman et al., 1988; Kellam and Larder, 1994; Luciw et al., 1995; Srinivasan et al., 1989; Velpandi et al., 1991). Recently, we applied IHR to generate a replication-competent SHIV carrying subtype C *env* that was inserted within the *env* sequence of subtype B (Fujita et al., 2013). Here, we utilized the same method to generate HIV-1mt by replacing a coding sequence region from subtype B with that of a primary isolate of subtype C and investigated recombination breakpoints in detail by analyzing the sequences of the resultant viruses. We found seven variants with different recombination breakpoints that were located within overlapped sequences between fragments I and II. These variants were selected as replication-competent virus in C8166-CCR5 cells that maintained their variability, suggesting that IHR events occur frequently in cells co-transfected with DNA fragments. In addition, it appears that the length of identical sequence of as short as 8 bp is sufficient for IHR (recombination type R2 in Fig. 4). Furthermore, IHR is suggested to occur between various DNA templates, based on the phylogenetic analysis results that indicated intermingled types of recombination breakpoints among different *env* sequences.

To develop a virus that efficiently infects monkey cells, it is important to choose an *env* that mediates efficient entry to macaque cells. The Env proteins in most A–D subtypes of HIV-1 clinical isolates from infected individuals during the acute phase of infection do not mediate efficient entry using macaque CD4 receptors (Humes et al., 2012). In a preliminary experiment in C8166-CCR5 cells, we generated five strains of replication-competent HIV-1mt carrying *env* from subtype C HIV-1 clinical isolates, including 97ZA012, but only three were infectious to PtM cells (data not shown). The generation of SHIV 97ZA012 that can establish infection in rhesus macaques as described previously (Fujita et al., 2013) also suggested that Env of HIV-1 97ZA012 can generate recombinant viruses that are infectious to macaque cells.

The serial passage of HIV-1mt ZA012-P0 through PtM PBMCs resulted in the loss of variants with recombination breakpoints and led to the emergence of HIV-1mt ZA012-P19 variants with shared uniform mosaic breakpoints not detected before the passage (Fig. 4). It is possible that recombination type R8 was generated through additional recombination events within homologous sequences in the *vpu* region between variants with recombination type R2 and R7 because recombinant breakpoints located on *vpr* and *env* regions of the virus were identical to that of R2 and R7, respectively. This possibility of recombination between R2 and R7 is also supported by the previous finding that the AAAAA tract within the putative site of recombination is a recombination hotspot during reverse transcription because the sequence facilitates template switching by pausing and dissociation of reverse transcriptase and results in frequent recombination (Quinones-Mateu et al., 2002).

HIV-1mt ZA012-P19 acquired three amino acid substitutions (K432R of Pol-RT, D232E of Pol-IN and F138S of Nef) through serial passages in PtM PBMCs, but the biological significance of these mutations remains undetermined. It has been reported previously that two amino acid substitutions (N222K and V234I) in the C-terminus of Pol-IN of NL4-3 could augment replication of HIV-1mt in cynomolgus macaque HSC-F and human MT4/CCR5 cells (Nomaguchi et al., 2013). A D232E mutation observed in this study was positioned near these two residues, which might be associated with increased replication in primate cells.

HIV-1mt ZA012 established infection in PtMs with the peak viremia reaching $1.0–2.3 \times 10^6$ copies/mL at 1.5 or 2 wpi (Fig. 7). In contrast, NL-DT5R exhibited low levels of replication in PtMs (at most 3.5×10^4 copies/mL at peak viremia) regardless of $CD8^+$ cell-depletion, as described previously (Igarashi et al., 2007). Plasma viral RNA load at peak viremia in HSIV-vif infected newborn PtMs showed $0.5–1.0 \times 10^5$ copies/mL (Thippeshappa et al., 2011). The highest peak viral level has been achieved by stHIV-1 infection of PtMs, reaching $1.0 \times 10^5–10^6$ copies/mL at the peak (Hatziioannou et al., 2009). Although HIV-1mt ZA012 failed to persist its replication over 10 weeks, the replication capacity of the virus in the acute phase appeared to be comparable to or greater than known monkey-tropic HIV-1 isolates. The caveat is that HIV-1mt ZA012 was obtained through "autologous" cell passage.

The derivative of NL-DT5R was designed to counteract or evade restrictions by macaque TRIM5α and APOBEC3G but not by interferon (IFN)-stimulated genes (ISGs). One of the IFNα-inducible host factors, tetherin, inhibits release of viral particles from infected cells (Neil et al., 2008). HIV-1 Vpu is able to counteract human tetherin activity but fails to downregulate this activity in macaque (Jia et al., 2009). On the other hand, unlike HIV-1 HXB2 or NL4-3, some strains of HIV-1 appear to antagonize macaque tetherin by its N-terminal transmembrane (TM) domain of Vpu (Shingai et al., 2011). It has been reported that replication of monkey-tropic HIV-1 could be controlled in macaque lymphocytes treated with IFN-α (Bitzegeio et al., 2013; Thippeshappa et al., 2013). Further investigations are required to determine whether HIV-1mt ZA012-P19 that encodes the N-terminal TM domain of Vpu, Env and Nef from subtype C could efficiently replicate in the presence of PtM tetherin or ISGs.

We generated the first CCR5-tropic HIV-1mt in the currently available derivatives of HIV-1 that can establish infection in macaques. NL-DT5R, HSIV-vif and stHIV-1 are infectious to PtMs, but these viruses are CXCR4 or CXCR4/CCR5 dual tropic. Several monkey-tropic HIV-1 isolates carrying CCR5-tropic *env* have been reported, but the viral replication was less efficient than NL-DT5R (Yamashita et al., 2008). The CCR5-tropic viruses preferentially infect memory $CD4^+$ T-lymphocytes and efficiently replicate in effector sites *in vivo* (i.e., lymphocytes in the lung or gastrointestinal tract) (Brenchley et al., 2004; Mehandru et al., 2004; Okoye et al., 2007; Picker et al., 2004). Although we characterized co-receptor usage of HIV-1mt ZA012-P19 *in vitro*, further investigation is needed to determine whether the virus behaves similarly to CCR5-tropic HIV-1 isolates in patients *in vivo*.

In this study, we generated a new monkey-tropic HIV-1. The viral swarm HIV-1mt ZA012-P19 carries *env* sequences from CCR5-tropic subtype C HIV-1, and it successfully established infection in PtMs with a high peak viremia comparable or greater than the monkey-tropic HIV-1 strains currently available. Although the monkey-tropic HIV-1 requires further adaptation to improve its *in vivo* replication capacity, the virus potentially serves as a nonhuman primate model for AIDS, which reproduces infection with currently circulating HIV-1.

Materials and methods

Cells

293 T cells (DuBridge et al., 1987) were maintained in Dulbecco's Modified Eagle Medium (D-MEM; Wako, Osaka, Japan) supplemented with 10% (vol/vol) fetal bovine serum (FBS; HyClone Laboratories, Logan, UT) and 1 mM L-glutamine. TZM-bl cells (Platt et al., 1998) from the NIH AIDS research and reference reagent program were maintained in D-MEM supplemented with 10% FBS, 1 mM L-glutamine and 1 mM sodium pyruvate. The human T-cell line, C8166-CCR5 (Shimizu et al., 2006) was maintained in Rosewell Park Memorial Institute 1640 medium (RPMI-1640; Invitrogen, Carlsbad, CA) supplemented with 10% FBS. PtM PBMCs from uninfected monkeys were isolated using the ficoll density gradient separation method. For this procedure, a mixture of 95% lymphocyte separation medium (Wako) and 5% phosphate buffered saline (PBS) was used as a separation solution as described previously (Agy et al., 1992; Frumkin et al., 1993). Residual erythrocytes were lysed in ACK lysing buffer (0.15 M NH_4Cl, 10 mM $KHCO_3$, 1.0 mM EDTA·Na_2). Depletion of $CD8^+$ cells was conducted with the magnetic-activated cell sorting (MACS) system (Miltenyi Biotec, Gladbach, Germany). Briefly, isolated PtM PBMCs were stained with phycoerythrin (PE)-conjugated anti-CD8 antibodies (clone SK1, BD Biosciences, San Jose, CA) and then labeled with anti-PE MicroBeads (Miltenyi Biotec). $CD8^+$ cells were removed using a magnetic column according to the manufacturer's instructions. PBMCs were cultured in RPMI-1640 supplemented with 10% FBS, 2 mM sodium pyruvate, 2 mM L-glutamine, 50 nM 2-mercaptoethanol and 40 μg/mL gentamicin. PBMCs were stimulated with 25 μg/mL Concanavalin A (conA) for 20 h and then cultured in the presence of 160 U/mL human recombinant interleukin-2 (IL-2; Wako).

Viruses

A stock of NL-DT5R virus was prepared from C8166-CCR5 cells transfected with a plasmid encoding full-length proviral DNA of NL-DT5R (pNL-DT5R) using the DEAE-Dextran/osmotic shock procedure (Takai and Ohmori, 1990). SIVmac239 (Kestler et al., 1988) stock virus was prepared from the culture supernatant of 293 T cells transfected with a plasmid encoding full-length proviral DNA of SIVmac239 with Lipofectamine (Invitrogen). CCR5-tropic subtype C HIV-1 clinical isolates including 97ZA012 were obtained from the NIH AIDS research and reference reagent program.

Generation of recombinant virus through intracellular homologous recombination

To generate recombinant virus by IHR, overlapping viral genomic DNA fragments were prepared by PCR amplification. A region spanning the 5′ LTR to *env* was amplified from pNL-DT5R (GenBank accession number: AB266485) using the HIV-1-U3-NotI-F forward primer (5′-ATGCGGCCGCTGGAAGGGCTAATTTGGTCCCAAAG-3′; nucleotide positions 1–25 in NL-DT5R, and additional *NotI* site sequences) and the env-2R reverse primer (5′-CACAGAGTGGGGTTAATTTTACAC-3′; nucleotide positions 6761–6784 in NL-DT5R). PCR was conducted with Expand long-range dNTPack (Roche Diagnostic, Basel, Switzerland). PCR conditions were as follows: 94 °C for 2 min followed by 10 cycles of 94 °C for 15 s, 55 °C for 30 s and 68 °C for 8 min, 25 cycles of 94 °C for 15 s, 55 °C for 30 s, 68 °C for 8 min, with 20 s increments at 68 °C for each successive cycle and a final elongation period of 68 °C for 7 min (fragment I in Fig. 1A). Amplification of a DNA fragment spanning the initiation of *vpr* to the 3′ LTR was derived from subtype C HIV-1 clinical isolates of the HIV-1 97ZA012 strain. Viral RNA was isolated from culture supernatant using a QIAamp viral RNA mini kit (Qiagen, Hilden, Germany). Complementary DNA (cDNA) was synthesized with Super Script III first-strand synthesis SuperMix (Invitrogen) using the OFM19-R reverse primer (5′-AGGCAAGCTTTATTGAGGCTTA-3′; nucleotide positions 9604–9625 based on the HXB2 numbering). PCR amplification of the viral cDNA was conducted using HIV-1vpr-F forward primer (5′-AGATGGAACAAGCCCCAGAAGA-3′; nucleotide positions 5558–5579 in the HXB2 numbering) and OFM19-R reverse primer with the same conditions (fragment II in Fig. 1A). To prepare a fragment spanning the initiation of 5′ LTR to the MA region of *gag*, proviral DNA was extracted from proviral DNA of subtype C HIV-1 isolate-infected C8166-CCR5 cells using DNeasy Blood & Tissue kits (Qiagen). The following amplification was conducted using HIV-1cladeC-U3-NotI-F forward primer (5′-ATGCGGCCGCTGGAAGGGTTAATTTACTCAAGAG-3′; nucleotide positions 1–24 in the HXB2 numbering plus *NotI* site sequences) and the PreSCA-R reverse primer (5′-AATCTATCCCATTCTGCAGC-3′; nucleotide positions 1433–1414 in the HXB2 numbering) (fragment III in Fig. 1A). The PCR products were purified using QIAquick PCR purification kits (Qiagen).

Recombinant viruses were generated by means of IHR in the cell. PCR-amplified linear viral DNA fragments were co-transfected into C8166-CCR5 cells by the DEAE-dextran/osmotic shock procedure (Takai and Ohmori, 1990). After transfection, cells were maintained and passaged every 3 days. The culture supernatant was harvested upon observation of virus-induced CPE.

Virus titration

The infectious titer of the viruses was defined as the median tissue culture infectious dose ($TCID_{50}$) in TZM-bl cells as described previously (Li et al., 2005). Four-fold, serially diluted viral stock was used to inoculated TZM-bl cells (5000 cells per 200 μL of growth medium containing DEAE-Dextran at a final concentration of 12.5 μg/mL) in quadruplicate in flat-bottom 96-well plates. After incubation for 48 h at 37 °C, the culture supernatant was removed and the cells were treated with 50 μL of Cell lysis solution (Toyo-Inki, Tokyo, Japan) for 15 min at room temperature with shaking. Then, 30 μL of the cell lysate were transferred to F96 MicroWell plates (Thermo Fisher Scientific, Roskilde, Denmark), and the relative luminescence units (RLU) after adding 50 μL of luciferase substrate (PicaGene, Toyo-Inki) to each well was determined using a microplate reader (Mithrus LB940, Berthold Technologies, Bad Wildbad, Germany). Viral infectivity was measured in RLUs, and positive wells were defined as RLU > 2 × background. The $TCID_{50}$ was calculated as described previously (Reed and Muench, 1938).

Viral growth kinetics in pig-tailed macaque PBMCs

PtM PBMCs were isolated from two uninfected animals and $CD8^+$ cells were depleted as described above. Two days after stimulation with Concanavarin A (25 μg/mL), 2.5×10^5 cells of $CD8^+$ cell-depleted PtM PBMCs were inoculated with 2.5×10^4 $TCID_{50}$ of viral stocks by spinoculation (O'Doherty et al., 2000) at 1200*g* for 1 h at room temperature. After washing with PBS, the infected cells in 200 μL of culture medium were cultured in round-bottom 96-well plates at 37 °C. The upper 150 μL of culture supernatant without aspirating cells in the bottom of the well was exchanged with fresh medium everyday. The harvested supernatant was stored at −20 °C prior to measure the activity of RT associated with virions.

RT assay

The virion-associated RT activity in culture supernatant was monitored as described previously (Willey et al., 1988). Briefly,

6 μL of culture supernatant were combined with 30 μL of RT reaction cocktail [50 mM Tris–HCl, 75 mM KCl, 10 mM dithiothreitol, 4.95 mM $MgCl_2$, 10 mg/mL polyA RNA, 5 mg/mL oligo-dT_{20}, 0.05% NP40] and 1.66×10^4 Bq equivalent α^{32}P-dTTP (PerkinElmer, Waltham, Massachusetts, USA) and incubated at 37 °C for 2 h with gentle agitation. Next, 3 μL of incubated mixture were blotted onto DE81 ion exchange cellulose paper (GE healthcare, Buckinghamshire, UK). After four washes with 2 × saline sodium citrate (SSC), the residual radioactivity from synthesized DNA was counted using a liquid scintillation counter.

Single genome amplification (SGA)

SGA of the region spanning the initiation region of *vpr* to the end of the *env* gene was conducted as described previously (Salazar-Gonzalez et al., 2008). Synthesized viral cDNA was end-point diluted and then subjected to nested-PCR. First-round PCR was conducted with KOD-FX (TOYOBO, Osaka, Japan) in a total of 20 μL of reaction mixture, using the SGA-16F forward primer (5′-TGCAGCAGAGTAATCTTCCCACTACAGG-3′; nucleotide positions 5260–5283 in NL-DT5R) and the SGA-OFM19R reverse primer (5′-AGGCAAGCTTTATTGAGGCTTAAGCAGTGG-3′; 9771–9800 in NL-DT5R). The first-round PCR conditions were as follows: 94 °C for 2 min, followed by 35 cycles of 98 °C for 10 s, 63 °C for 30 s and 68 °C for 5 min. Second-round PCR was performed using 1 μL of the first-round PCR product using the SGA-17F forward primer (5′-AGAAGAGACAATAGGAGAGGCCTTCGAATG-3′; 5610–5639 in NL-DT5R) and the SGA-2.5R reverse primer (5′-AAAGCAGCTGCTTATATGCAGCATCTGAGG-3′; 9673–9702 in NL-DT5R). The second-round PCR conditions were the same as those in the first-round PCR. Amplification of the target sequence was confirmed with agarose gel electrophoresis. According to a Poisson distribution, when a positive ratio of amplification from diluted cDNA is $< 30\%$ in multiple replicate PCR reactions, the amplicons are predicted to be amplified from one-copy of template with the probability of $> 80\%$. The single genome amplicons were purified before sequence analysis.

Genomic analysis

Sequence analysis was performed using the BigDye terminator v. 3.1 cycle sequencing kit (Applied Biosystems, Foster City, CA) and the ABI PRISM 3130xl genetic analyzer (Applied Biosystems). The 3′-terminal 2304 nucleotide sequences of *env* were aligned using the Clustal X software (Thompson et al., 1997). A neighbor-joining phylogenetic tree (Saitou and Nei, 1987) using Kimura's two-parameter model (Kimura, 1980) was constructed using MEGA 5 software (Tamura et al., 2011), and bootstrap values were computed from 1000 bootstrap replicates (Felsenstein, 1985). Pair-wise distances between any two nucleic acid sequences of the 3′ terminal 2361 bp of each viral *env* within the parental HIV-1 97ZA012, HIV-1mt ZA012-P0 and HIV-1mt ZA012-P19 were calculated with Kimura's two-parameter model (Kimura, 1980) by using MEGA 5 software (Tamura et al., 2011). The statistical significance between each viral pair-wise distance was calculated with Student's *t* test using GraphPad Prism software (San Diego, CA, USA).

Co-receptor usage assay

Employing a previously reported method (Nishimura et al., 2010) with minor modifications, co-receptor usage of viruses was determined using the small molecule antagonists, AD101 (Trkola et al., 2002) provided by Dr. Julie Strizki (Schering-Plough Research Institute, Kenilworth, NJ) and AMD3100 (Sigma-Aldrich, St. Louis, MO) (Donzella et al., 1998). Briefly, freshly trypsinized TZM-bl cells (5000 cells per 100 μL of growth medium containing DEAE-Dextran at a final concentration of 12.5 μg/mL) were seeded in flat-bottom 96-well plates. The cells were incubated with 50 μL of co-receptor antagonists at final concentrations ranging from 0.1 nM to 1000 nM for 1 h at 37 °C and inoculated with 100 $TCID_{50}$ of replication-competent virus in triplicate. After incubation for 48 h at 37 °C, luciferase activity was measured, and the percent infectivity relative to that measured in mock-treated wells was determined.

Experimental infection of pig-tailed macaques with HIV-1mt ZA012

HIV-1mt ZA012 challenge stock was prepared from culture supernatant of PtM PBMCs infected with HIV-1mt ZA012-P19. The virus was titrated with PtM PBMCs as described previously (Fujita et al., 2013). Two pig-tailed macaques, PtM01 and PtM02 aged 7 and 6 years, respectively, were intravenously inoculated with 1.0×10^5 $TCID_{50}$ of HIV-1mt ZA012. Plasma viral RNA loads were measured with TaqMan real time RT-PCR as described previously (Miyake et al., 2006) with minor modifications; RT-PCR was conducted for HIV-1 *vpr* amplification using the NM3rNvpr-F forward primer (5′-CAGAAGACCAAGGGCCACAG-3′) and NM3rNvpr-R reverse primer (5′-GTCTAACAGCTTCACTCTTAAGTTCCTCT-3′). PCR products were detected with a labeled probe, NM3rNvpr-T (5′-Fam-AGGGAGCCATACAATGAATGGACACT-Tamra-3′; Perkin Elmer). Animal experiments were conducted in the biosafety level 3 animal facility, in compliance with institutional regulations approved by the Committee for Experimental Use of Nonhuman Primates of the Institute for Virus Research, Kyoto University, Kyoto, Japan.

Flow cytometry

To enumerate $CD4^+$ T-lymphocytes, and memory and naïve $CD4^+$ T-lymphocytes, whole blood samples were stained with fluorescently labeled mouse monoclonal antibodies. Anti-CD3 (clone SP34-2) conjugated with Pacific Blue, anti-CD4 (clone L200) conjugated with PerCP-Cy5.5, anti-CD8 (clone SK1) conjugated with APC-Cy7, anti-CD20 (clone L27) conjugated with FITC and anti-CD95 (clone DX2) conjugated with APC were purchased from BD Biosciences, and anti-CD28 (clone CD28.2) conjugated with PE was purchased from eBioscience (San Diego, CA). $CD28^{high}CD95^{low}CD4^+$ or $CD28^{high/low}CD95^{high}CD4^+$ T-cell subsets were considered as naïve or memory $CD4^+$ T-lymphocytes, respectively (Pitcher et al., 2002). The absolute number of lymphocytes in the blood was determined using an automated hematology analyzer, KX-21 (Sysmex, Kobe, Japan).

Acknowledgments

The authors thank Akio Adachi for providing plasmid DNA encoding the full-length sequence of NL-DT5R; Drs. Julie Strizki and Paul Zavodny of the Schering-Plough Research Institute, Kenilworth, NJ, USA, for providing AD101; the NIH AIDS Research & Reference Reagent Program for providing primary isolates of HIV-1 and TZM-bl cells; Kenta Matsuda for helpful discussion; former and current members of the Igarashi Laboratory for discussion and support with animal procedures and analyses. This work was supported by a Research on HIV/AIDS grant (H21-AIDS Research-008, H22-AIDS Research-007, H24-AIDS Research-008 and H25-AIDS Research-009) from The Ministry of Health, Labor and Welfare of Japan, and by a Grant-in-Aid for Scientific Research (B) (21300152, 23300156 and 26290032) and Grant-in-Aid for challenging Exploratory Research (23658240) from the Japan Society for the Promotion of Science.

References

Agy, M.B., Frumkin, L.R., Corey, L., Coombs, R.W., Wolinsky, S.M., Koehler, J., Morton, W.R., Katze, M.G., 1992. Infection of *Macaca nemestrina* by human immunodeficiency virus type-1. Science 257, 103–106.

Berthoux, L., Sebastian, S., Sokolskaja, E., Luban, J., 2005. Cyclophilin A is required for TRIM5 α-mediated resistance to HIV-1 in Old World monkey cells. Proc. Nat. Acad. Sci. U.S.A. 102, 14849–14853.

Bitzegeio, J., Sampias, M., Bieniasz, P.D., Hatziioannou, T., 2013. Adaptation to the interferon-induced antiviral state by human and simian immunodeficiency viruses. J. Virol. 87, 3549–3560.

Brenchley, J.M., Schacker, T.W., Ruff, L.E., Price, D.A., Taylor, J.H., Beilman, G.J., Nguyen, P.L., Khoruts, A., Larson, M., Haase, A.T., Douek, D.C., 2004. $CD4^+$ T cell depletion during all stages of HIV disease occurs predominantly in the gastrointestinal tract. J. Exp. Med. 200, 749–759.

Brennan, G., Kozyrev, Y., Hu, S.-L., 2008. TRIMCyp expression in Old World primates *Macaca nemestrina* and *Macaca fascicularis*. Proc. Nat. Acad. Sci. U.S.A. 105, 3569–3574.

Chen, Z., Huang, Y., Zhao, X., Skulsky, E., Lin, D., Ip, J., Gettie, A., Ho, D.D., 2000. Enhanced infectivity of an R5-tropic simian/human immunodeficiency virus carrying human immunodeficiency virus type 1 subtype C envelope after serial passages in pig-tailed macaques (*Macaca nemestrina*). J. Virol. 74, 6501–6510.

Choe, H., Farzan, M., Sun, Y., Sullivan, N., Rollins, B., Ponath, P.D., Wu, L., Mackay, C.R., LaRosa, G., Newman, W., Gerard, N., Gerard, C., Sodroski, J., 1996. The beta-chemokine receptors CCR3 and CCR5 facilitate infection by primary HIV-1 isolates. Cell 85, 1135–1148.

Choisy, M., Woelk, C.H., Guegan, J.F., Robertson, D.L., 2004. Comparative study of adaptive molecular evolution in different human immunodeficiency virus groups and subtypes. J. Virol. 78, 1962–1970.

Donzella, G.A., Schols, D., Lin, S.W., Este, J.A., Nagashima, K.A., Maddon, P.J., Allaway, G.P., Sakmar, T.P., Henson, G., De Clercq, E., Moore, J.P., 1998. AMD3100, a small molecule inhibitor of HIV-1 entry via the CXCR4 co-receptor. Nat. Med. 4, 72–77.

Doranz, B.J., Rucker, J., Yi, Y., Smyth, R.J., Samson, M., Peiper, S.C., Parmentier, M., Collman, R.G., Doms, R.W., 1996. A dual-tropic primary HIV-1 isolate that uses fusin and the beta-chemokine receptors CKR-5, CKR-3, and CKR-2b as fusion cofactors. Cell 85, 1149–1158.

DuBridge, R.B., Tang, P., Hsia, H.C., Leong, P.M., Miller, J.H., Calos, M.P., 1987. Analysis of mutation in human cells by using an Epstein-Barr virus shuttle system. Mol. Cell Biol. 7, 379–387.

Felsenstein, J., 1985. Confidence limits on phylogenies: an approach using the bootstrap. Evolution 39, 783–791.

Feng, Y., Broder, C.C., Kennedy, P.E., Berger, E.A., 1996. HIV-1 entry cofactor: functional cDNA cloning of a seven-transmembrane, G protein-coupled receptor. Science 272, 872–877.

Freed, E.O., Martin, M.A., 1996. Domains of the human immunodeficiency virus type 1 matrix and gp41 cytoplasmic tail required for envelope incorporation into virions. J. Virol. 70, 341–351.

Frumkin, L.R., Agy, M.B., Coombs, R.W., Panther, L., Morton, W.R., Koehler, J., Florey, M.J., Dragavon, J., Schmidt, A., Katze, M.G., et al., 1993. Acute infection of *Macaca nemestrina* by human immunodeficiency virus type 1. Virology 195, 422–431.

Fujita, Y., Otsuki, H., Watanabe, Y., Yasui, M., Kobayashi, T., Miura, T., Igarashi, T., 2013. Generation of a replication-competent chimeric simian-human immunodeficiency virus carrying *env* from subtype C clinical isolate through intracellular homologous recombination. Virology 436, 100–111.

Gaschen, B., Taylor, J., Yusim, K., Foley, B., Gao, F., Lang, D., Novitsky, V., Haynes, B., Hahn, B.H., Bhattacharya, T., Korber, B., 2002. Diversity considerations in HIV-1 vaccine selection. Science 296, 2354–2360.

Gibbs, R.A., Rogers, J., Katze, M.G., Bumgarner, R., Weinstock, G.M., Mardis, E.R., Remington, K.A., Strausberg, R.L., Venter, J.C., Wilson, R.K., Batzer, M.A., Bustamante, C.D., Eichler, E.E., Hahn, M.W., Hardison, R.C., Makova, K.D., Miller, W., Milosavljevic, A., Palermo, R.E., Siepel, A., Sikela, J.M., Attaway, T., Bell, S., Bernard, K.E., Buhay, C.J., Chandrabose, M.N., Dao, M., Davis, C., Delehaunty, K.D., Ding, Y., Dinh, H.H., Dugan-Rocha, S., Fulton, L.A., Gabisi, R.A., Garner, T.T., Godfrey, J., Hawes, A.C., Hernandez, J., Hines, S., Holder, M., Hume, J., Jhangiani, S.N., Joshi, V., Khan, Z.M., Kirkness, E.F., Cree, A., Fowler, R.G., Lee, S., Lewis, L.R., Li, Z., Liu, Y.S., Moore, S.M., Muzny, D., Nazareth, L.V., Ngo, D.N., Okwuonu, G.O., Pai, G., Parker, D., Paul, H.A., Pfannkoch, C., Pohl, C.S., Rogers, Y.H., Ruiz, S.J., Sabo, A., Santibanez, J., Schneider, B.W., Smith, S.M., Sodergren, E., Svatek, A.F., Utterback, T.R., Vattathil, S., Warren, W., White, C.S., Chinwalla, A.T., Feng, Y., Halpern, A.L., Hillier, L.W., Huang, X., Minx, P., Nelson, J.O., Pepin, K.H., Qin, X., Sutton, G.G., Venter, E., Walenz, B.P., Wallis, J.W., Worley, K.C., Yang, S.P., Jones, S.M., Marra, M.A., Rocchi, M., Schein, J.E., Baertsch, R., Clarke, L., Csuros, M., Glasscock, J., Harris, R.A., Havlak, P., Jackson, A.R., Jiang, H., Liu, Y., Messina, D.N., Shen, Y., Song, H.X., Wylie, T., Zhang, L., Birney, E., Han, K., Konkel, M.K., Lee, J., Smit, A.F., Ullmer, B., Wang, H., Xing, J., Burhans, R., Cheng, Z., Karro, J.E., Ma, J., Raney, B., She, X., Cox, M.J., Demuth, J.P., Dumas, L.J., Han, S.G., Hopkins, J., Karimpour-Fard, A., Kim, Y.H., Pollack, J.R., Vinar, T., Addo-Quaye, C., Degenhardt, J., Denby, A., Hubisz, M.J., Indap, A., Kosiol, C., Lahn, B.T., Lawson, H.A., Marklein, A., Nielsen, R., Vallender, E.J., Clark, A.G., Ferguson, B., Hernandez, R.D., Hirani, K., Kehrer-Sawatzki, H., Kolb, J., Patil, S., Pu, L.L., Ren, Y., Smith, D.G., Wheeler, D.A., Schenck, I., Ball, E.V., Chen, R., Cooper, D.N., Giardine, B., Hsu, F., Kent, W.J., Lesk, A., Nelson, D.L., O'Brien, W.E., Prufer, K., Stenson, P.D., Wallace, J.C., Ke, H., Liu, X.M., Wang, P., Xiang, A.P., Yang, F., Barber, G.P., Haussler, D., Karolchik, D., Kern, A.D., Kuhn, R.M., Smith, K.E., Zwieg, A.S., 2007. Evolutionary and biomedical insights from the rhesus macaque genome. Science 316, 222–234.

Gnanakaran, S., Lang, D., Daniels, M., Bhattacharya, T., Derdeyn, C.A., Korber, B., 2007. Clade-specific differences between human immunodeficiency virus type 1 clades B and C: diversity and correlations in C3-V4 regions of gp120. J. Virol. 81, 4886–4891.

Goff, S.P., 2007. Retroviridae: the retroviruses and their replication. In: Knipe, D.M., Howley, P.M. (Eds.), Fields Virology, fifth ed. Lippincott Williams & Wilkins, Philadelphia, PA.

Goulder, P.J., Watkins, D.I., 2004. HIV and SIV CTL escape: implications for vaccine design. Nat. Rev. Immunol. 4, 630–640.

Harouse, J.M., Gettie, A., Tan, R.C.H., Blanchard, J., Cheng-Mayer, C., 1999. Distinct pathogenic sequela in rhesus macaques infected with CCR5 or CXCR4 utilizing SHIVs. Science 284, 816–819.

Hatziioannou, T., Ambrose, Z., Chung, N.P., Piatak Jr., M., Yuan, F., Trubey, C.M., Coalter, V., Kiser, R., Schneider, D., Smedley, J., Pung, R., Gathuka, M., Estes, J.D., Veazey, R.S., KewalRamani, V.N., Lifson, J.D., Bieniasz, P.D., 2009. A macaque model of HIV-1 infection. Proc. Nat. Acad. Sci. U.S.A. 106, 4425–4429.

Hatziioannou, T., Princiotta, M., Piatak, M., Yuan, F., Zhang, F., Lifson, J.D., Bieniasz, P.D., 2006. Generation of simian-tropic HIV-1 by restriction factor evasion. Science 314, 95.

Hemelaar, J., 2012. The origin and diversity of the HIV-1 pandemic. Trends Mol. Med. 18, 182–192.

Humes, D., Emery, S., Laws, E., Overbaugh, J., 2012. A species-specific amino acid difference in the macaque CD4 receptor restricts replication by global circulating HIV-1 variants representing viruses from recent infection. J. Virol. 86, 12472–12483.

Igarashi, T., Iyengar, R., Byrum, R.A., Buckler-White, A., Dewar, R.L., Buckler, C.E., Lane, H.C., Kamada, K., Adachi, A., Martin, M.A., 2007. Human immunodeficiency virus type 1 derivative with 7% simian immunodeficiency virus genetic content is able to establish infections in pig-tailed macaques. J. Virol. 81, 11549–11552.

Javaherian, K., Langlois, A.J., Schmidt, S., Kaufmann, M., Cates, N., Langedijk, J.P., Meloen, R.H., Desrosiers, R.C., Burns, D.P., Bolognesi, D.P., et al., 1992. The principal neutralization determinant of simian immunodeficiency virus differs from that of human immunodeficiency virus type 1. Proc. Nat. Acad. Sci. U.S.A. 89, 1418–1422.

Jia, B., Serra-Moreno, R., Neidermyer, W., Rahmberg, A., Mackey, J., Fofana, I.B., Johnson, W.E., Westmoreland, S., Evans, D.T., 2009. Species-specific activity of SIV Nef and HIV-1 Vpu in overcoming restriction by tetherin/BST2. PLoS Pathog. 5, e1000429.

Kalyanaraman, S., Jannoun-Nasr, R., York, D., Luciw, P.A., Robinson, R., Srinivasan, A., 1988. Homologous recombination between human immunodeficiency viral DNAs in cultured human cells: analysis of the factors influencing recombination. Biochem. Biophys. Res. Commun. 157, 1051–1060.

Kamada, K., Igarashi, T., Martin, M.A., Khamsri, B., Hatcho, K., Yamashita, T., Fujita, M., Uchiyama, T., Adachi, A., 2006. Generation of HIV-1 derivatives that productively infect macaque monkey lymphoid cells. Proc. Nat. Acad. Sci. U.S.A. 103, 16959–16964.

Kanki, P.J., McLane, M.F., King Jr., N.W., Letvin, N.L., Hunt, R.D., Sehgal, P., Daniel, M.D., Desrosiers, R.C., Essex, M., 1985. Serologic identification and characterization of a macaque T-lymphotropic retrovirus closely related to HTLV-III. Science 228, 1199–1201.

Keckesova, Z., Ylinen, L.M., Towers, G.J., 2006. Cyclophilin A renders human immunodeficiency virus type 1 sensitive to Old World monkey but not human TRIM5 alpha antiviral activity. J. Virol. 80, 4683–4690.

Kellam, P., Larder, B.A., 1994. Recombinant virus assay: a rapid, phenotypic assay for assessment of drug susceptibility of human immunodeficiency virus type 1 isolates. Antimicrob. Agents Chemother. 38, 23–30.

Kestler 3rd, H.W., Li, Y., Naidu, Y.M., Butler, C.V., Ochs, M.F., Jaenel, G., King, N.W., Daniel, M.D., Desrosiers, R.C., 1988. Comparison of simian immunodeficiency virus isolates. Nature 331, 619–622.

Kiepiela, P., Ngumbela, K., Thobakgale, C., Ramduth, D., Honeyborne, I., Moodley, E., Reddy, S., de Pierres, C., Mncube, Z., Mkhwanazi, N., Bishop, K., van der Stok, M., Nair, K., Khan, N., Crawford, H., Payne, R., Leslie, A., Prado, J., Prendergast, A., Frater, J., McCarthy, N., Brander, C., Learn, G.H., Nickle, D., Rousseau, C., Coovadia, H., Mullins, J.I., Heckerman, D., Walker, B.D., Goulder, P., 2007. $CD8^+$ T-cell responses to different HIV proteins have discordant associations with viral load. Nat. Med. 13, 46–53.

Kimura, M., 1980. A simple method for estimating evolutionary rates of base substitutions through comparative studies of nucleotide sequences. J. Mol. Evol. 16, 111–120.

Kuiken, C.L., Foley, B., Guzman, E., Korber, B.T., 1999. Determinants of HIV-1 protein evolution. In: Crandall, K.A. (Ed.), Molecular Evolution of HIV. Johns Hopkins University Press, Baltimore MD.

Li, M., Gao, F., Mascola, J.R., Stamatatos, L., Polonis, V.R., Koutsoukos, M., Voss, G., Goepfert, P., Gilbert, P., Greene, K.M., Bilska, M., Kothe, D.L., Salazar-Gonzalez, J.F., Wei, X., Decker, J.M., Hahn, B.H., Montefiori, D.C., 2005. Human immunodeficiency virus type 1 env clones from acute and early subtype B infections for standardized assessments of vaccine-elicited neutralizing antibodies. J. Virol. 79, 10108–10125.

Luciw, P.A., Pratt-Lowe, E., Shaw, K.E., Levy, J.A., Cheng-Mayer, C., 1995. Persistent infection of rhesus macaques with T-cell-line-tropic and macrophage-tropic clones of simian/human immunodeficiency viruses (SHIV). Proc. Nat. Acad. Sci. U.S.A. 92, 7490–7494.

Mariani, R., Chen, D., Schrofelbauer, B., Navarro, F., Konig, R., Bollman, B., Munk, C., Nymark-McMahon, H., Landau, N.R., 2003. Species-specific exclusion of APOBEC3G from HIV-1 virions by Vif. Cell 114, 21–31.

Mehandru, S., Poles, M.A., Tenner-Racz, K., Horowitz, A., Hurley, A., Hogan, C., Boden, D., Racz, P., Markowitz, M., 2004. Primary HIV-1 infection is associated with preferential depletion of CD4+ T lymphocytes from effector sites in the gastrointestinal tract. J. Exp. Med. 200, 761–770.
Miyake, A., Ibuki, K., Enose, Y., Suzuki, H., Horiuchi, R., Motohara, M., Saito, N., Nakasone, T., Honda, M., Watanabe, T., Miura, T., Hayami, M., 2006. Rapid dissemination of a pathogenic simian/human immunodeficiency virus to systemic organs and active replication in lymphoid tissues following intrarectal infection. J. Gen. Virol. 87, 1311–1320.
Moore, P.L., Gray, E.S., Choge, I.A., Ranchobe, N., Mlisana, K., Abdool Karim, S.S., Williamson, C., Morris, L., 2008. The C3-V4 region is a major target of autologous neutralizing antibodies in human immunodeficiency virus type 1 subtype C infection. J. Virol. 82, 1860–1869.
Moore, P.L., Ranchobe, N., Lambson, B.E., Gray, E.S., Cave, E., Abrahams, M.R., Bandawe, G., Mlisana, K., Abdool Karim, S.S., Williamson, C., Morris, L., 2009. Limited neutralizing antibody specificities drive neutralization escape in early HIV-1 subtype C infection. PLoS Pathog. 5, e1000598.
Murphey-Corb, M., Martin, L.N., Rangan, S.R., Baskin, G.B., Gormus, B.J., Wolf, R.H., Andes, W.A., West, M., Montelaro, R.C., 1986. Isolation of an HTLV-III-related retrovirus from macaques with simian AIDS and its possible origin in asymptomatic mangabeys. Nature 321, 435–437.
Ndung'u, T., Lu, Y., Renjifo, B., Touzjian, N., Kushner, N., Pena-Cruz, V., Novitsky, V.A., Lee, T.H., Essex, M., 2001. Infectious simian/human immunodeficiency virus with human immunodeficiency virus type 1 subtype C from an African isolate: rhesus macaque model. J. Virol. 75, 11417–11425.
Neil, S., Bieniasz, P., 2009. Human immunodeficiency virus, restriction factors, and interferon. J. Interferon Cytokine Res. 29, 569–580.
Neil, S.J., Zang, T., Bieniasz, P.D., 2008. Tetherin inhibits retrovirus release and is antagonized by HIV-1 Vpu. Nature 451, 425–430.
Nishimura, Y., Igarashi, T., Donau, O.K., Buckler-White, A., Buckler, C., Lafont, B.A., Goeken, R.M., Goldstein, S., Hirsch, V.M., Martin, M.A., 2004. Highly pathogenic SHIVs and SIVs target different $CD4^+$ T cell subsets in rhesus monkeys, explaining their divergent clinical courses. Proc. Nat. Acad. Sci. U.S.A. 101, 12324–12329.
Nishimura, Y., Shingai, M., Willey, R., Sadjadpour, R., Lee, W.R., Brown, C.R., Brenchley, J.M., Buckler-White, A., Petros, R., Eckhaus, M., Hoffman, V., Igarashi, T., Martin, M.A., 2010. Generation of the pathogenic R5-tropic simian/human immunodeficiency virus SHIVAD8 by serial passaging in rhesus macaques. J. Virol. 84, 4769–4781.
Nomaguchi, M., Doi, N., Fujiwara, S., Saito, A., Akari, H., Nakayama, E.E., Shioda, T., Yokoyama, M., Sato, H., Adachi, A., 2013. Systemic biological analysis of the mutations in two distinct HIV-1mt genomes occurred during replication in macaque cells. Microb. Infect./Inst. Pasteur 15, 319–328.
O'Doherty, U., Swiggard, W.J., Malim, M.H., 2000. Human immunodeficiency virus type 1 spinoculation enhances infection through virus binding. J. Virol. 74, 10074–10080.
Okoye, A., Meier-Schellersheim, M., Brenchley, J.M., Hagen, S.I., Walker, J.M., Rohankhedkar, M., Lum, R., Edgar, J.B., Planer, S.L., Legasse, A., Sylwester, A.W., Piatak Jr., M., Lifson, J.D., Maino, V.C., Sodora, D.L., Douek, D.C., Axthelm, M.K., Grossman, Z., Picker, L.J., 2007. Progressive CD4+ central memory T cell decline results in CD4+ effector memory insufficiency and overt disease in chronic SIV infection. J. Exp. Med. 204, 2171–2185.
Picker, L.J., Hagen, S.I., Lum, R., Reed-Inderbitzin, E.F., Daly, L.M., Sylwester, A.W., Walker, J.M., Siess, D.C., Piatak Jr., M., Wang, C., Allison, D.B., Maino, V.C., Lifson, J.D., Kodama, T., Axthelm, M.K., 2004. Insufficient production and tissue delivery of CD4+ memory T cells in rapidly progressive simian immunodeficiency virus infection. J. Exp. Med. 200, 1299–1314.
Pitcher, C.J., Hagen, S.I., Walker, J.M., Lum, R., Mitchell, B.L., Maino, V.C., Axthelm, M.K., Picker, L.J., 2002. Development and homeostasis of T cell memory in rhesus macaque. J. Immunol. 168, 29–43.
Platt, E.J., Wehrly, K., Kuhmann, S.E., Chesebro, B., Kabat, D., 1998. Effects of CCR5 and CD4 cell surface concentrations on infections by macrophagetropic isolates of human immunodeficiency virus type 1. J. Virol. 72, 2855–2864.
Quinones-Mateu, M.E., Gao, Y., Ball, S.C., Marozsan, A.J., Abraha, A., Arts, E.J., 2002. *In vitro* intersubtype recombinants of human immunodeficiency virus type 1: comparison to recent and circulating *in vivo* recombinant forms. J. Virol. 76, 9600–9613.
Reed, L.J., Muench, H., 1938. A simple method of estimating fifty percent endpoints. Am. J. Hyg. 27, 493–497.
Reimann, K.A., Li, J.T., Veazey, R., Halloran, M., Park, I.-W., Karlsson, G.B., Sodroski, J., Letvin, N., 1996. A chimeric simian/human immunodeficiency virus expressing a primary patient human immunodeficiency vrus type 1 isolate *env* causes an AIDS-like disease after *in vivo* passage in rhesus monkeys. J. Virol. 70, 6922–6928.
Ren, W., Mumbauer, A., Gettie, A., Seaman, M.S., Russell-Lodrigue, K., Blanchard, J., Westmoreland, S., Cheng-Mayer, C., 2013. Generation of lineage-related, mucosally transmissible subtype C R5 simian-human immunodeficiency viruses capable of AIDS development, induction of neurological disease, and coreceptor switching in rhesus macaques. J. Virol. 87, 6137–6149.
Saitou, N., Nei, M., 1987. The neighbor-joining method: a new method for reconstructing phylogenetic trees. Mol. Biol. Evol. 4, 406–425.
Salazar-Gonzalez, J.F., Bailes, E., Pham, K.T., Salazar, M.G., Guffey, M.B., Keele, B.F., Derdeyn, C.A., Farmer, P., Hunter, E., Allen, S., Manigart, O., Mulenga, J., Anderson, J.A., Swanstrom, R., Haynes, B.F., Athreya, G.S., Korber, B.T., Sharp, P.M., Shaw, G.M., Hahn, B.H., 2008. Deciphering human immunodeficiency virus type 1 transmission and early envelope diversification by single-genome amplification and sequencing. J. Virol. 82, 3952–3970.
Sheehy, A.M., Gaddis, N.C., Choi, J.D., Malim, M.H., 2002. Isolation of a human gene that inhibits HIV-1 infection and is suppressed by the viral Vif protein. Nature 418, 646–650.
Shibata, R., Adachi, A., 1992. SIV/HIV recombinants and their use in studying biological properties. AIDS Res. Hum. Retroviruses 8, 403–409.
Shimizu, Y., Okoba, M., Yamazaki, N., Goto, Y., Miura, T., Hayami, M., Hoshino, H., Haga, T., 2006. Construction and *in vitro* characterization of a chimeric simian and human immunodeficiency virus with the RANTES gene. Microb. Infect./Inst. Pasteur 8, 105–113.
Shingai, M., Yoshida, T., Martin, M.A., Strebel, K., 2011. Some human immunodeficiency virus type 1 Vpu proteins are able to antagonize macaque BST-2 *in vitro* and *in vivo*: Vpu-negative simian-human immunodeficiency viruses are attenuated *in vivo*. J. Virol. 85, 9708–9715.
Song, R.J., Chenine, A.L., Rasmussen, R.A., Ruprecht, C.R., Mirshahidi, S., Grisson, R.D., Xu, W., Whitney, J.B., Goins, L.M., Ong, H., Li, P.L., Shai-Kobiler, E., Wang, T., McCann, C.M., Zhang, H., Wood, C., Kankasa, C., Secor, W.E., McClure, H.M., Strobert, E., Else, J.G., Ruprecht, R.M., 2006. Molecularly cloned SHIV-1157ipd3N4: a highly replication- competent, mucosally transmissible R5 simian-human immunodeficiency virus encoding HIV clade C Env. J. Virol. 80, 8729–8738.
Srinivasan, A., York, D., Jannoun-Nasr, R., Kalyanaraman, S., Swan, D., Benson, J., Bohan, C., Luciw, P.A., Schnoll, S., Robinson, R.A., Desai, S.M., Devare, S.G., 1989. Generation of hybrid human immunodeficiency virus by homologous recombination. Proc. Nat. Acad. Sci. U.S.A. 86, 6388–6392.
Stremlau, M., Owens, C.M., Perron, M.J., Kiessling, M., Autissier, P., Sodroski, J., 2004. The cytoplasmic body component TRIM5alpha restricts HIV-1 infection in Old World monkeys. Nature 427, 848–853.
Stremlau, M., Perron, M., Lee, M., Li, Y., Song, B., Javanbakht, H., Diaz-Griffero, F., Anderson, D.J., Sundquist, W.I., Sodroski, J., 2006. Specific recognition and accelerated uncoating of retroviral capsids by the TRIM5alpha restriction factor. Proc. Nat. Acad. Sci. U.S.A. 103, 5514–5519.
Takai, T., Ohmori, H., 1990. DNA transfection of mouse lymphoid cells by the combination of DEAE-dextran-mediated DNA uptake and osmotic shock procedure. Biochim. Biophys. Acta 1048, 105–109.
Tamura, K., Peterson, D., Peterson, N., Stecher, G., Nei, M., Kumar, S., 2011. MEGA5: molecular evolutionary genetics analysis using maximum likelihood, evolutionary distance, and maximum parsimony methods. Mol. Biol. Evol. 28, 2731–2739.
Thippeshappa, R., Polacino, P., Yu Kimata, M.T., Siwak, E.B., Anderson, D., Wang, W., Sherwood, L., Arora, R., Wen, M., Zhou, P., Hu, S.L., Kimata, J.T., 2011. Vif substitution enables persistent infection of pig-tailed macaques by human immunodeficiency virus type 1. J. Virol. 85, 3767–3779.
Thippeshappa, R., Ruan, H., Wang, W., Zhou, P., Kimata, J.T., 2013. A variant macaque-tropic human immunodeficiency virus type 1 is resistant to alpha interferon-induced restriction in pig-tailed macaque CD4+ T cells. J. Virol. 87, 6678–6692.
Thompson, J.D., Gibson, T.J., Plewniak, F., Jeanmougin, F., Higgins, D.G., 1997. The CLUSTAL_X windows interface: flexible strategies for multiple sequence alignment aided by quality analysis tools. Nucleic Acids Res. 25, 4876–4882.
Trkola, A., Kuhmann, S.E., Strizki, J.M., Maxwell, E., Ketas, T., Morgan, T., Pugach, P., Xu, S., Wojcik, L., Tagat, J., Palani, A., Shapiro, S., Clader, J.W., McCombie, S., Reyes, G.R., Baroudy, B.M., Moore, J.P., 2002. HIV-1 escape from a small molecule, CCR5-specific entry inhibitor does not involve CXCR4 use. Proc. Nat. Acad. Sci. U.S.A. 99, 395–400.
Velpandi, A., Nagashunmugam, T., Murthy, S., Cartas, M., Monken, C., Srinivasan, A., 1991. Generation of hybrid human immunodeficiency virus utilizing the cotransfection method and analysis of cellular tropism. J. Virol. 65, 4847–4852.
Willey, R.L., Smith, D.H., Lasky, L.A., Theodore, T.S., Earl, P.L., Moss, B., Capon, D.J., Martin, M.A., 1988. *in vitro* mutagenesis identifies a region within the envelope gene of the human immunodeficiency virus that is critical for infectivity. J. Virol. 62, 139–147.
Yamashita, T., Doi, N., Adachi, A., Nomaguchi, M., 2008. Growth ability in simian cells of monkey cell-tropic HIV-1 is greatly affected by downstream region of the vif gene. J. Med. Invest.: JMI 55, 236–240.

frontiers in
MICROBIOLOGY

EDITORIAL
published: 03 December 2014
doi: 10.3389/fmicb.2014.00672

Animal model studies on viral infections

Akio Adachi[1]* and Tomoyuki Miura[2]

[1] *Department of Microbiology, Institute of Health Biosciences, The University of Tokushima Graduate School, Tokushima, Japan*
[2] *Laboratory of Primate Model, Experimental Research Center for Infectious Diseases, Institute for Virus Research, Kyoto University, Kyoto, Japan*
**Correspondence: adachi@basic.med.tokushima-u.ac.jp*

Edited by:
Akihide Ryo, Yokohama City University, Japan

Reviewed by:
Yasuo Ariumi, Kumamoto University, Japan
Ayumi Kudoh, Yokohama City University School of Medicine, Japan

Keywords: animal models, viral infections, viral replication, viral pathogenicity, anti-viral strategies

One of the major missions of animal virology is to understand how viruses replicate and cause asymptomatic/symptomatic conditions in individuals (Nomaguchi and Adachi, 2010). It is especially important for virologists who work on viruses pathogenic for humans to elucidate bases underlying the *in vivo* viral characteristics. Toward this end, animal model studies in some ways are necessary to precisely analyze the *in vivo* situation, and also are essential for developing countermeasures against virus infections. Since a full variety of viruses with distinct biological properties exist, we virologists should study "the target virus" in a specialized manner, in addition to common theoretical/experimental approaches. The Research Topic entitled "Animal model studies on viral infections" collects articles that describe the studies on numerous virus species for their animal models, or those at various stages toward animal experiments.

Articles in this Research Topic were written by experts in various research fields, and can be fairly grouped into a few categories: (i) descriptions/evaluations/new challenges of animal model studies for investigating the biology of viruses; (ii) experimental materials/methods for upcoming animal model studies; (iii) observations important for animal model studies. (i) Reynaud and Horvat (2013) have described the animal models for human herpesvirus 6 to better understand its pathogenic property. Studies on filoviruses, classified as biosafety level-4 and represent a serious world-wide problem today, have been reviewed by Nakayama and Saijo (2013). Mailly et al. (2013) have focused on the quest for appropriate animal models for hepatitis C virus. Clark et al. (2013) have discussed about the use of non-human primates as models for dengue hemorrhagic fever/dengue shock syndrome. Ohsugi (2013) has summarized mouse strains transgenic for the *tax* gene of human T-cell leukemia virus type 1 (HTLV-1). Also, a bovine model for HTLV-1 pathogenesis has been described by Aida et al. (2013). Challenging new attempts to establish human immunodeficiency virus type 1 (HIV-1)/macaque infection models have been reviewed by Misra et al. (2013), and also by Saito and Akari (2013). Another approach to understand HIV-1 biology *in vivo* has been described by Matsuyama-Murata et al. (2013). (ii) Kodama et al. (2013) has described a new and simple method to prepare human dendritic cells from peripheral blood mononuclear cells. Doi et al. (2013) have summarized their studies on macaque-tropic HIV-1 clones. Ikeno et al. (2013) has reported a new, sensitive, and quantitative system to monitor measles virus infection in humanized mice. Iwami et al. (2013) have summarized the quantification of viral infection dynamics based on various quantitative analyses. (iii) Tada et al. (2013) have suggested that LEDGF/p75 may be a cellular factor acting as a species-barrier against HIV-1 in mouse cells. Kuwata et al. (2013) have shown that simian immunodeficiency virus may acquire the increased infectivity and resistance to neutralizing antibodies by truncation of its gp41 cytoplasmic tail. Ohsugi et al. (2013) have reported that natural infection status of laboratory mice by murine norovirus. Finally, Kajitani et al. (2013) have described the possible involvement of E1^E4 protein of human papillomavirus type 18 in its differentiation-dependent life cycle.

We are proud to add our "Animal model studies on viral infections" to a series of Research Topic in Frontiers in Microbiology. A wide variety of DNA and RNA viruses are covered by this special issue consisting of original research, review, mini-review, methods, and opinion articles. As we described in the beginning, animal studies are certainly required for understanding virus replicative/pathogenic properties *in vivo* and for overcoming virally-caused infectious diseases. We human virologists should make every effort to fight against numbers of unique pathogenic viruses.

REFERENCES

Aida, Y., Murakami, H., Takagashi, M., and Takeshima, S. (2013). Mechanisms of pathogenesis induced by bovine leukemia virus as a model for huma T-cell leukemia virus. *Front. Microbiol.* 4:328. doi: 10.3389/fmicb.2013.00328

Clark, K., Onlamoon, N., Hsiao, H.-M., Perng, G., and Villinger, F. (2013). Can non-huma primates serve as models for investigating dengue disease pathogenesis? *Front. Microbiol.* 4:305. doi: 10.3389/fmicb.2013.00305

Doi, N., Okubo, A., Yamane, M., Sakai, Y., Adachi, A., and Nomaguchi, M. (2013). Growth potentials of CCR5-tropic/CXCR4-tropic HIV-1mt clones in macaque cells. *Front. Microbiol.* 4:2188. doi: 10.3389/fmicb.2013.00218

Ikeno, S., Suzuki, M., Muhsen, M., Ishige, M., Kobayashi, M., Ohno, S., et al. (2013). Sensitive detection of measles virus infection in the blood and tissues of humanized mouse by one-step quantitative RT-PCR. *Front. Microbiol.* 4:298. doi: 10.3389/fmicb.2013.00298

Iwami, S., Koizumi, Y., Ikeda, H., and Kakizoe, Y. (2013). Quantification of viral infection dynamics in animal experiments. *Front. Microbiol.* 4:264. doi: 10.3389/fmicb.2013.002264

Kajitani, N., Satsuka, A., Yoshida, S., and Sakai, K. (2013). HPV 18 E1^E4 is assembled into aggresome-like compartment and involved in sequestration

of viral oncoproteins. *Front. Microbiol.* 4:251. doi: 10.3389/fmicb.2013.00251

Kodama, A., Tanaka, R., Saito, M., Ansari, A., and Tanaka, Y. (2013). A novel and simple method for generation of human dendritic cells from unfractionated peripheral blood mononuclear cells within 2 days: its application for induction of HIV-1-reactive $CD4^+$ T cells in the hu-PBL SCID mice. *Front. Microbiol.* 4:292. doi: 10.3389/fmicb.2013.00292

Kuwata, T., Takaki, K., Enomoto, I., Yoshimura, K., and Matsushita, S. (2013). Increased infectivity in human cells and resistance to antibody-mediated neutralization by truncation of the SIV gp41 cytoplasmic tail. *Front. Microbiol.* 4:117. doi: 10.3389/fmicb.2013.00117

Mailly, L., Robinet, E., Meuleman, P., Baumert, T. F., and Zeisel, M. B. (2013). Hepatitis C virus infection and related liver disease: the quest for the best animal model. *Front. Microbiol.* 4:212. doi: 10.3389/fmicb.2013.00212

Matsuyama-Murata, M., Inaba, K., Horiuchi, R., Fukazawa, Y., Ibuki, K., Hayami, M., et al. (2013). Genetic similarity of circulating and small intestinal virus at the end stage of acute pathogenic simian-human immunodeficiency virus infection. *Front. Microbiol.* 4:204. doi: 10.3389/fmicb.2013.00204

Misra, A., Thippeshappa, R., and Kimata, J. T. (2013). Macaques as model hosts for studies of HIV-1 infection. *Front. Microbiol.* 4:176. doi: 10.3389/fmicb.2013.00176

Nakayama, E., and Saijo, M. (2013). Animal models for Ebola and Marburg virus infections. *Front. Microbiol.* 4:267. doi: 10.3389/fmicb.2013.00267

Nomaguchi, M., and Adachi, A. (2010). Virology as biosystematics: towards understanding the viral infection biology. *Front. Microbiol.* 1:2. doi: 10.3389/fmicb.2010.00002

Ohsugi, T. (2013). A transgenic mouse model of huma T cell leukemia virus type 1-associated diseases. *Front. Microbiol.* 4:49. doi: 10.3389/fmicb.2013.00049

Ohsugi, T., Matsuura, K., Kawabe, S., Nakamura, N., Kumar, J. M., Wakamiya, M., et al. (2013). Natural infection of murine norovirus in conventional and specific pathogen-free laboratory mice. *Front. Microbiol.* 4:12. doi: 10.3389/fmicb.2013.00012

Reynaud, J., and Horvat, B. (2013). Animal models for human herpesvirus 6 infection. *Front. Microbiol.* 4:174. doi: 10.3389/fmicb.2013.00174

Saito, A., and Akari, H. (2013). Macaque-tropic human immunodeficiency virus type 1: breaking out of the host restriction factors. *Front. Microbiol.* 4:187. doi: 10.3389/fmicb.2013.00187

Tada, T., Kadoki, M., Yang, L., Tokunaga, K., and Iwakura, Y. (2013). Transgenic expression of the human LEDGF/p75 gene relieves the species barrier against HIV-1 infection in mouse cells. *Front. Microbiol.* 4:377. doi: 10.3389/fmicb.2013.00377

Conflict of Interest Statement: The authors declare that the research was conducted in the absence of any commercial or financial relationships that could be construed as a potential conflict of interest.

Received: 03 November 2014; accepted: 19 November 2014; published online: 03 December 2014.

Citation: Adachi A and Miura T (2014) Animal model studies on viral infections. Front. Microbiol. 5:672. doi: 10.3389/fmicb.2014.00672

This article was submitted to Virology, a section of the journal Frontiers in Microbiology.

ELSEVIER

Institut Pasteur

Microbes and Infection xx (2013) 1–8

www.elsevier.com/locate/micinf

Original article

Cross-reactivity analysis of T cell receptors specific for overlapping HIV-1 Nef epitopes of different lengths

Chihiro Motozono [a,1], Masaru Yokoyama [b], Hironori Sato [b], Takamasa Ueno [a,*]

[a] *Center for AIDS Research, Kumamoto University, Kumamoto, Japan*
[b] *Laboratory of Viral Genomics, Pathogen Genomics Center, National Institute of Infectious Diseases, Tokyo, Japan*

Received 1 November 2013; accepted 22 December 2013

Abstract

Overlapping peptides of different lengths from a certain immunodominant region can be presented by the same HLA class I molecule and elicit different T cell responses. However, how peptide-length specificity of antigen-specific $CD8^+$ T lymphocytes influence cross-reactivity profiles of these cells remains elusive. This question is particularly important in the face of highly variable pathogens such as HIV-1. Here, we examined this problem by using HLA-B*35:01-restricted $CD8^+$ T lymphocytes specific for Nef epitopes, i.e., RY11 (RPQVPLRPMTY), VY8 (VPLRPMTY), and RM9 (RPQVPLRPM), in which VY8 and RM9 were contained entirely within RY11, in combination with a T cell receptor (TCR) reconstruction system as well as HLA-B35 tetramers and a set of a single-variant peptide library. The TCR reactivity toward the peptide-length variants was classified into three types: mutually exclusive specificity toward (1) RY11 or (2) VY8 and (3) cross-recognition toward RM9 and RY11. TCR cross-reactivity toward variant peptides was similar within the same peptide-length reactivity type but was markedly different between the types. Thus, TCRs showing similar peptide-length reactivity have shared peptide recognition footprints and thereby similar weakness to antigenic variations, providing us with further insight into the antiviral vaccine design.

Keywords: HIV-1; $CD8^+$ T cell; TCR; Antigenic peptide; Cross-reactivity; HLA-B*35:01

1. Introduction

HLA class I (HLA-I) molecules form a highly polymorphic antigen-binding cleft and play a central role in selection and presentation of antigenic peptides to T lymphocytes. Crystal structures of HLA-I in complex with an antigenic peptide have shown that the central residues in the peptide are generally exposed at the outside of the HLA binding groove, thus affording recognition by cognate T cell receptors (TCRs) [1]. The fixed anchors at the N- and C-termini of the antigenic peptide of 8-13 amino acids in length, and the closed conformation of the HLA-I groove, force longer peptides to bulge further out of the groove to accommodate the extra central peptide residues [2]. Such a difference in peptide conformation as well as the size of the central bulge bound to HLA substantially influences the TCR selection and recognition [3]. The same HLA-I molecule can eventually present various closely related overlapping peptides of different lengths [4], while closely related HLA-I allomorphs have different length preference toward overlapping epitopes in some settings that result in qualitatively variable T cell-mediated viral control [5–9].

Viruses such as the highly variable HIV-1 and hepatitis C viruses can mutate and thus escape from CTL responses [10,11], and it is becoming evident that CTLs with the capacity to cross-recognize naturally occurring viral variants are advantageous for viral control *in vivo* [12–17]. In a region of viral proteins where multiple overlapping epitopes of various length are clustering, a mutation results in a change in multiple

* Corresponding author. Center for AIDS Research, Kumamoto University, 2-2-1 Chuo-ku, Honjo, Kumamoto 860-0811, Japan. Tel.: +81 96 373 6826; fax: +81 96 373 6825.
E-mail address: uenotaka@kumamoto-u.ac.jp (T. Ueno).
[1] Present address: Department of Immunology, Kinki University School of Medicine, Osaka, Japan.

1286-4579/$ - see front matter © 2013 Institut Pasteur. Published by Elsevier Masson SAS. All rights reserved.
http://dx.doi.org/10.1016/j.micinf.2013.12.005

Please cite this article in press as: Motozono C, et al., Cross-reactivity analysis of T cell receptors specific for overlapping HIV-1 Nef epitopes of different lengths, Microbes and Infection (2013), http://dx.doi.org/10.1016/j.micinf.2013.12.005

epitopes and may differentially influence T cell responses specific for such epitopes [5]. This case is likely where an HLA-I allomorph presents multiple overlapping epitopes of different length. However, how such overlapping peptides of different lengths presented by the same HLA allele affect length preference and cross-reactive potency of TCRs toward variant peptides remains unclear.

In HIV-1 Nef, a highly immunogeneic viral protein, a number of CTL epitopes are located within a multi-restricted, immunodominant central region spanning residues 73-94 and 113-147, including a highly conserved polyproline region at residues 73-82 [18,19]. In particular, HLA-B*35:01, which prefers proline at the second position of its bound peptides [19,20], can present multiple overlapping epitopes within this region, leading to elicitation of different antigen-specific CTL responses [5,6,19,20]. In fact, we previously reported that in HIV-infected patients with HLA-B*35:01, Nef protein elicited dominant CTL responses [21], with a short epitope (VY8; VPLRPMTY) and an amino-terminal extended long epitope (RY11; RPQVPLRPMTY) being different optimal epitopes presented by HLA-B*35:01 [5,6]. There is also another potential epitopic peptide sequence, RM9 (RPQVPLRPM), within RY11. In this present study, employing TCR-reconstructed T cells, we carefully investigated peptide-length preferences of various TCRs and examined whether, and if so how, cross-reactivity profiles of these TCRs were affected by peptide-length preference.

2. Materials and Methods

2.1. Reagents

HLA-B35 tetramers in complex with the RY11, RM9 or VY8 peptides were prepared as previously described [21]. Peptides were designed based on the subtype B consensus sequence of HIV-1 Nef (see Los Alamos database at http://www.hiv.lanl.gov/content/index) and were prepared by using an automated multiple peptide synthesizer. The purity and integrity of the synthesized peptides was examined by high-performance liquid chromatography and mass spectrometry, and the peptides with >90% purity were used in this study. Antibodies used were the following: PE-conjugated anti-mouse CD3ε mAb (2C11: BioLegend), anti-human CD8-PerCP (BD Biosciences), and anti-human CD3-FITC (DakoCytomation).

2.2. CTL clones

CTL clones that had been established by using PBMC samples taken from HLA-B*35:01$^+$ individuals (Pt-01, -03, -19, and -33) with an HIV-1 infection were used [5,6,21]. CTL clone H231 generated from PBMC from Pt-01 was designated CTL 01-H231, and other clones were similarly designated. Cytotoxic assays were done as previously described [5,6,21]. The study was conducted in accordance with the human experimentation guidelines of Kumamoto University.

2.3. TCR reconstruction

TCR-encoding genes of CTL clones were obtained by using a SMART PCR cDNA synthesis kit (Clontech, Palo Alto, CA) as described previously [22,23]. The resultant TCR αβ genes were separately cloned into a retrovirus vector pMX (provided by T. Kitamura at Tokyo University) and delivered into a TCR-deficient mouse T cell hybridoma cell line, TG40 (provided by T. Saito at RIKEN Institute), as previously described [6,22]. The human CD8α gene was similarly delivered into the cells as needed. TG40 cells transduced with TCR genes isolated from CTL 01-H231 were designated TG40-H231 and other TCR-transduced cells were similarly designated.

TCR recognition of cognate antigens was measured in terms of IL-2 secretion by TCR-transduced TG40 cells, as described earlier [6,22]. Unless otherwise specified, C1R cells expressing HLA-B*35:01 (C1R-B3501, 10^4 cells/well), TCR-transduced TG40 cells (2×10^4 cells/well), and peptides were mixed and incubated for 24 h at 37 °C. The resultant culture supernatant was then collected, and the amount of IL-2 was determined by analyzing the proliferative activity of the IL-2 indicator cell line CTLL-2.

2.4. Flow cytometric analysis

CTL clones were stained with PE- or allophycocyanin-labeled HLA-B35 tetramers at 37 °C for 15 min followed by incubation with anti-CD8-PerCP and anti-CD3-FITC at 4 °C for 15 min. By flow cytometry, CD3$^+$ CD8$^+$ live cells were gated and analyzed for tetramer binding, as described previously [6]. TCR-reconstructed TG40 cells were stained with HLA-B35 tetramers at 4 °C for 15 min followed by anti-CD3-PE at 4 °C for 20 min. By flow cytometry, CD3$^+$ live cells were gated and analyzed for tetramer binding as described earlier [6,22]. Cells were analyzed by use of a FACS Calibur or FACS Canto II flow cytometer (BD Biosciences), and the data were further analyzed by using Flow Jo (Treestar, San Diego CA).

2.5. Structural modeling of pMHC

The crystal structure of HLA-B*35:01 with the VY8 peptide at a resolution of 2.00 Å (PDB code: 1A1N [24]) was taken from the Protein Data Bank to construct the complexes between HLA-B*35:01 and RM9 or RY11. The modeling was performed by using tools available in the Molecular Operating Environment (MOE, MOE 2012.1001; Chemical Computing Group Inc., Montreal, Quebec, Canada) as follows: First, hydrogen was added to the HLA structure. The HLA-B*35:01 structure was thermodynamically optimized by energy minimization using MOE and an AMBER12EHT force field [25] combined with the generalized Born model of aqueous solvation implemented in MOE [26]. Next, the RM9 or RY11 peptide models on the HLA-B*35:01 structure were constructed by the homology modeling technique using 'MOE-Homology' in MOE. Finally, the RM9 or RY11 model was

Please cite this article in press as: Motozono C, et al., Cross-reactivity analysis of T cell receptors specific for overlapping HIV-1 Nef epitopes of different lengths, Microbes and Infection (2013), http://dx.doi.org/10.1016/j.micinf.2013.12.005

docked with the HLA-B*35:01 structures by using the automated ligand docking program ASEDock [27] operated in MOE.

3. Results

3.1. Multiple overlapping epitopic sequences in Nef in the context of HLA-B*35:01

In the HLA-B*35:01-restricted epitopic peptide sequence RPQVPLRPMTY (RY11), located in the immunodominant central region of Nef (Fig. 1), there are two additional sequences, VPLRPMTY (VY8) and RPQVPLRPM (RM9), that have similar motifs for HLA-B*35:01 binding, i.e., Pro at position 2 (P2) and a hydrophobic residue at the C-terminus [19–21]. In fact, RY11 [21,28] and VY8 [5,29] have been reported as CTL epitopes presented by HLA-B*35:01, although RM9 is not yet known to be an HLA-B*35:01-restricted epitope. The results of an HLA-stabilization assay showed that RM9 bound to HLA-B*35:01 with a half maximal binding level (BL_{50}) of 22 μM, which is comparable to that of RY11 (23 μM) and VY8 (41 μM), suggesting that RM9 could also be presented by HLA-B*35:01 for TCR recognition. Corroboratively, the peptide replacement structural modeling studies showed that RM9 could be accommodated in the peptide-binding groove of HLA-B*35:01, as could RY11 and VY8 (Fig. 1). Also, VY8, RM9, and RY11 peptides each had a distinct surface area available for TCR binding (Fig. 1).

Because $CD8^+$ T lymphocytes have preference toward peptide-length variants [3,8,9,21,30,31], we tested again a panel of CTL clones (CTL01-H231, CTL03-G8, CTL19-27, CTL19-139, and CTL33-S1) for cytotoxic activity toward cells pulsed with VY8, RM9 or RY11 peptides. All CTL clones showed cytotoxic activity toward target cells pulsed with RY11 (Fig. 2A), suggesting that RY11 contained antigenic determinants recognized by all of these TCRs, which would be consistent with previous studies [6,21]. However, CTL19-139 and CTL33-S1 showed more potent activity toward cells pulsed with VY8 than with RY11 and no response toward cells pulsed with RM9 (Fig. 2A). In support of this finding, these clones showed binding exclusively to VY8/B35 tetramers and not to RM9/B35 or RY11/B35 tetramers (Fig. 2B), indicating that CTL19-139 and CTL33-S1 were exclusively specific for VY8. CTL01-H231 did not show cytotoxic activity toward cells pulsed with RM9 or VY8 (Fig. 2A). In fact, CTL01-H231 bound exclusively to RY11/B35 tetramers, but not to RM9/B35 or VY8/B35 ones (Fig. 2B), indicating that CTL01-H231 was exclusively specific for RY11. On the other hand, CTL03-G8 and CTL19-27 showed cytotoxic activity toward cells pulsed with both RM9 and RY11; although at a lower peptide concentration these clones showed about 10 times more potent activity toward RM9- than toward RY11-pulsed cells (Fig. 2A). Consistently, CTL03-G8 and CTL19-27 exhibited higher binding activity toward the RM9/B35 tetramer than toward the RY11/B35 one (Fig. 2B), suggesting that RM9 could be an epitope for these CTLs.

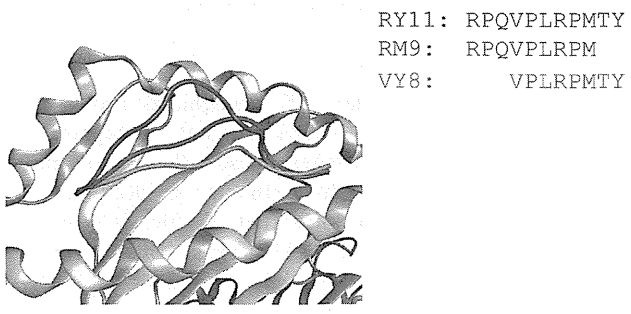

Fig. 1. Structural modeling of HLA-B*35:01 in complex with RY11, RM9 or VY8. The HLA-B*35:01-peptide complex models were constructed by using the crystal structures of HLA-B*35:01 in complex with VY8 at a resolution of 2.00 Å (PDB code: 1A1N [24]), as described in Materials and Methods. RY11 (blue) and RM9 (magenta) are superimposed on the VY8 (cyan) peptide-HLA-B*35:01 model.

3.2. Fine specificity analysis by use of TCR-reconstructed cells

To certify fine specificity and peptide-length preference of the above CTLs, TCRs isolated from these CTLs were reconstructed on TCR-deficient T cell line TG40 cells; because this method allowed us to precisely examine the TCR-peptide-MHC interaction without any influence of functional differences among primary CTLs [6,22,23]. By introduction of TCR genes into TG40 cells (designated TG40-H231, TG40-G8, TG40-27, TG40-139, and TG40-S1), TCR/CD3 expression was clearly observed in all cells (Fig. 3A), confirming TCR reconstruction on the TG40 cell surface. We next tested the TCR specificity by peptide titration and tetramer staining. We confirmed that TG40-139 and S1 efficiently recognized target cells pulsed with the VY8 peptide and bound to VY8/B35 tetramers (Fig. 3B and C), in good agreement with the CTL data shown in Fig. 2. As expected, TG40-H231 exclusively recognized target cells pulsed with RY11 (Fig. 3B) and bound to the RY11/B35 tetramer but not to the RM9/B35 tetramer (Fig. 3C). On the other hand, TG40-G8 and TG40-27 responded towards cells pulsed with both RM9 and RY11 without much difference in sensitivity in the peptide titration experiments (Fig. 3B); whereas both cells showed a different pattern of tetramer binding (Fig. 3C). TG40-G8 showed substantial binding activity toward RM9/B35 tetramers (Fig. 3C), but weak binding activity toward RY11/B35 ones (Fig. 3C). In contrast, TG40-27 showed extremely weak or virtually no binding to RY11/B35 or RM9/B35 tetramers (Fig. 3C), although CTL19-27 bound to both tetramers (Fig. 2B). Taken together, these data indicate that TCRs that favorably recognized RM9 also cross-recognized RY11 in the context of HLA-B*35:01, at least to some extent.

3.3. Cross-reactivity profiles of TCRs towards an array of variant peptides

We next analyzed TCR cross-reactivity towards 198 RY11-based variant peptides. Overall, TG40-H231, TG40-

Please cite this article in press as: Motozono C, et al., Cross-reactivity analysis of T cell receptors specific for overlapping HIV-1 Nef epitopes of different lengths, Microbes and Infection (2013), http://dx.doi.org/10.1016/j.micinf.2013.12.005

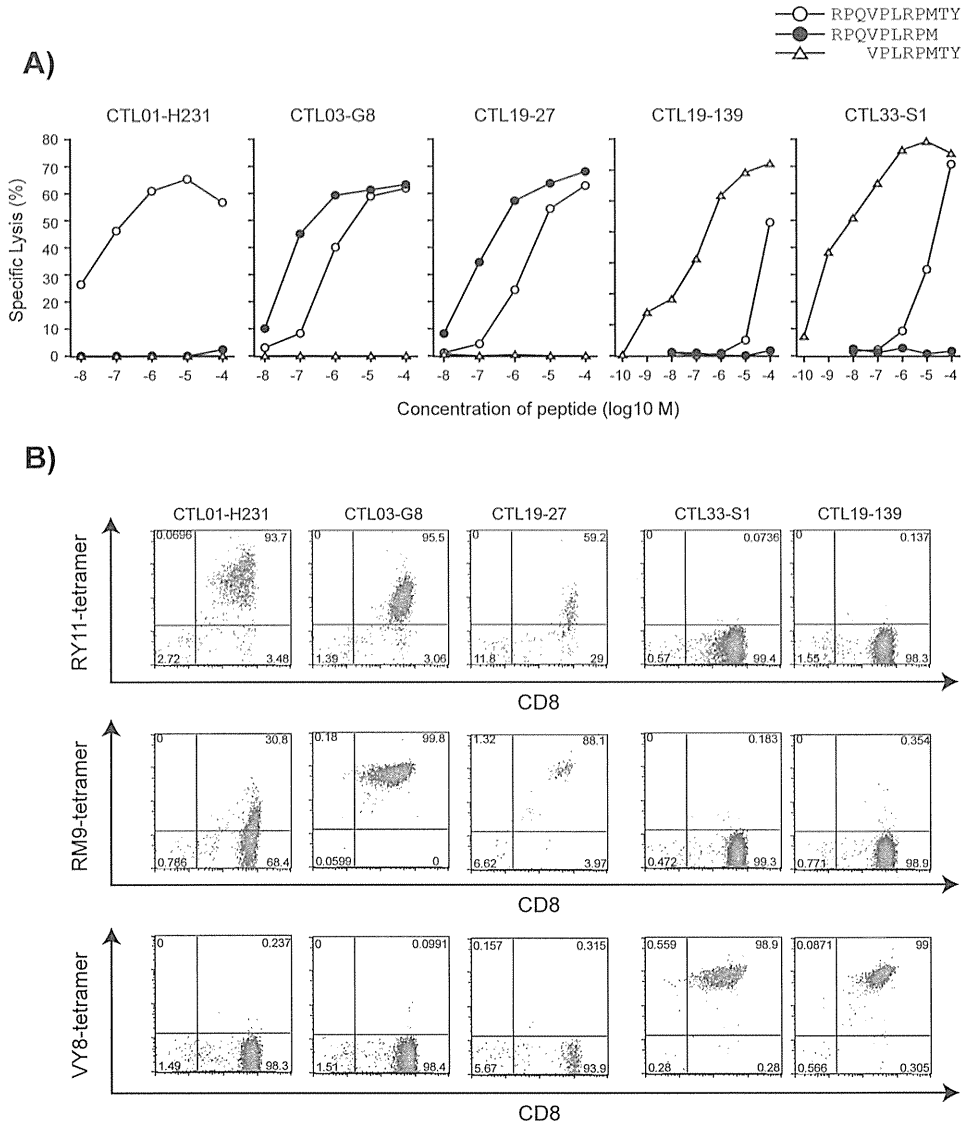

Fig. 2. Specificity of CTL clones toward overlapping epitopic peptides. A) Cytotoxic activity of CTL clones (CTL01-H231, CTL03-G8, CTL19-27, CTL19-139, and CTL33-S1) toward overlapping peptides is shown. As target cells, C1R cells expressing HLA-B*35:01 (C1R-B3501) were pulsed with various concentrations of RY11, RM9 or VY8 peptides. Data presented are the mean of duplicate assays. B) CTL clones were stained with HLA-B35 tetramers in complex with RY11, RM9 or VY8. Live $CD3^+$ cells were gated and analyzed for antigen specificity by binding with HLA-B35 tetramers.

G8, and TG40-27 retained reactivity towards 72, 45, and 46 out of the 198 variant peptides tested (36.4%, 22.7%, and 23.2% recognition, respectively; Fig. 4). Interestingly, although TG40-G8 and TG40-27 showed cross-reactivity towards only some amino acid variations at P1-P9, they showed cross-reactivity toward most amino acid residues at P10 and P11, suggesting that these peptides likely bound to HLA-B*35:01 with extending two amino acids at the C-terminus from the peptide-binding region, rather than their central region bulging for TCR-binding, as shown previously from crystal structural data [7,32]. This observation was consistent with the length preference of RM9 peptide by these TCRs, as was shown above. However, it is not clear why neither TG40-G8 nor -27 recognized Pro at P10 (Fig. 4). In contrast, TG40-H231 efficiently recognized all mutations at P8 of RY11, whereas these cells showed limited cross-recognition toward hydrophobic residues at P11 (Fig. 4). We also tested cross-reactivity profiles of TG40-139 and TG40-S1 by using 144 RY11-variant peptides containing mutations from P4 to P11, which corresponded to P1 to P8 of the VY8 sequence. TG40-139 and TG40-S1 showed unique cross-reactivity footprints compared with the other TCRs tested. All these data suggest that TCRs having similar peptide-length preference showed cross-recognition patterns related to the amino acid variations in the epitope peptides.

Please cite this article in press as: Motozono C, et al., Cross-reactivity analysis of T cell receptors specific for overlapping HIV-1 Nef epitopes of different lengths, Microbes and Infection (2013), http://dx.doi.org/10.1016/j.micinf.2013.12.005

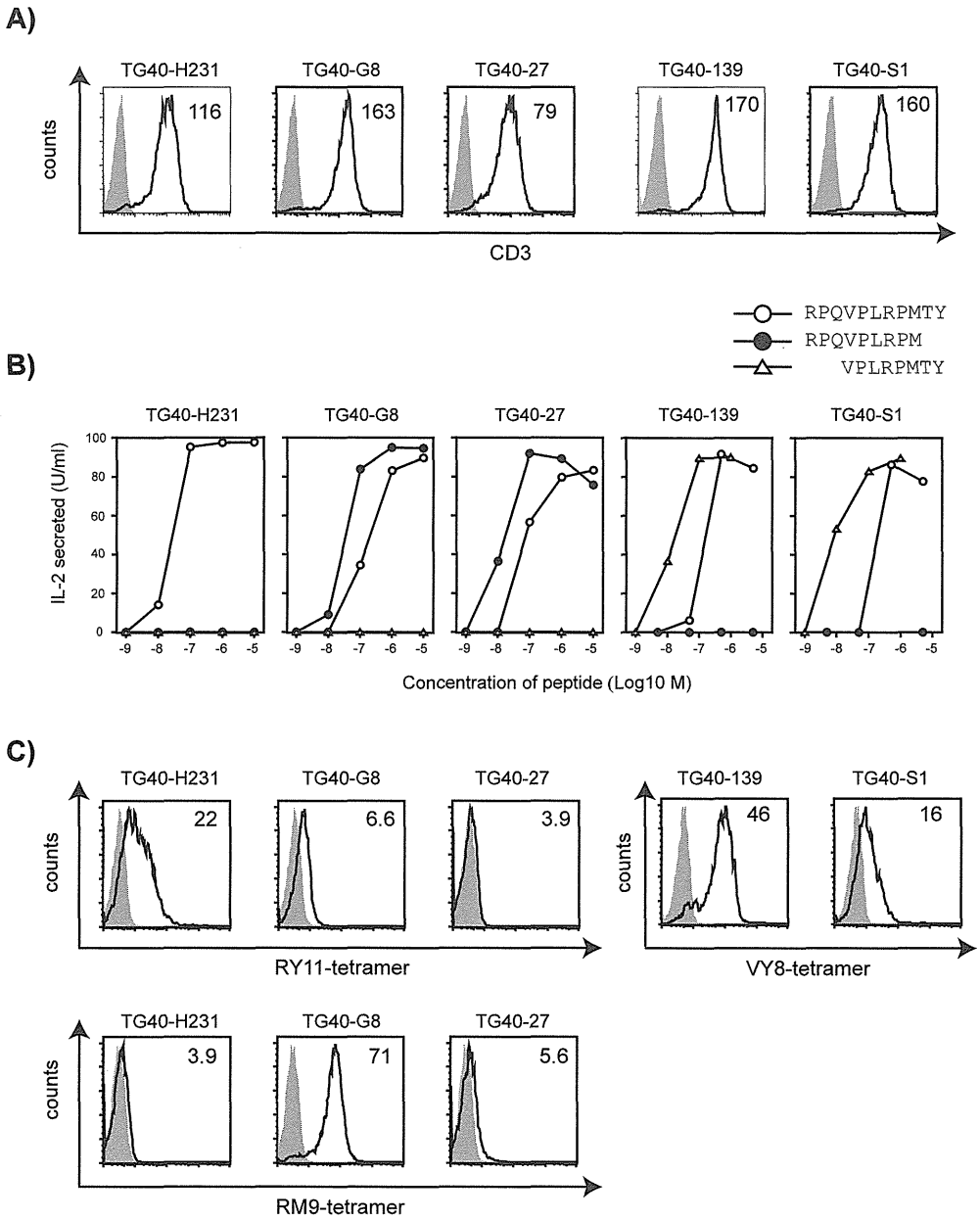

Fig. 3. Specificity analysis of reconstructed TCRs from H231, G8, 27, 139, and S1 CTL clones were reconstructed on TCR-deficient TG40 cells. A) Cell-surface expression of reconstructed TCRs was evaluated by staining with PE-conjugated anti-mouse CD3e mAb. The mean fluorescence intensity of CD3 expression is indicated in each histogram. The mock-transduced TG40 cells were used as a negative control (shaded). B) TG40/CD8 cells expressing the indicated TCRs were analyzed for their IL-2 secretion in response to various concentrations of the RY11, RM9 or VY8 peptides. The amount of IL-2 obtained for the mock-transduced TG40/CD8 was always <2.0. This assay was repeated three to four times for each peptide. C) HLA tetramer binding activity of TCR-transduced TG40 cells was analyzed. The mean fluorescence intensity of HLA tetramers is indicated in each histogram. The mock-transduced TG40 cells were used as a negative control (shaded), and the mean fluorescence intensity of these cells was <3.2.

4. Discussion

Here, we highlighted TCR fine specificity and cross-reactivity toward peptide-length variants as well as amino acid variations within the defined length of three HIV-1 Nef peptides by using a number of TCRs restricted by the same HLA-I molecule, HLA-B*35:01. Tetramer and peptide titration assays in combination with the TCR-reconstruction system revealed that the length preference of TCRs could be categorized into three types: mutually exclusive specificity toward RY11 or VY8 and cross-recognition toward RM9 and RY11. In addition, the cross-reactivity profiles toward amino acid variations of TCRs were unique and shared within the length-preference type but were very different between the

Please cite this article in press as: Motozono C, et al., Cross-reactivity analysis of T cell receptors specific for overlapping HIV-1 Nef epitopes of different lengths, Microbes and Infection (2013), http://dx.doi.org/10.1016/j.micinf.2013.12.005

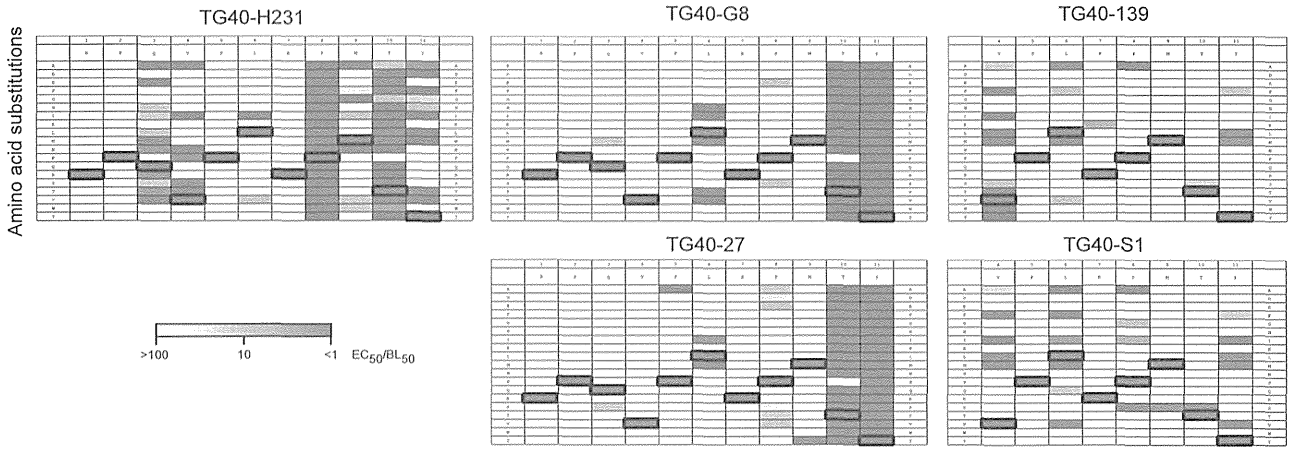

Fig. 4. Cross-reactivity footprints of TG40/CD8 cells expressing the indicated TCRs were tested for their capacity to recognize C1R-B3501 pulsed with each of 198 different peptides. The amino acid in each of the eleven positions in the RPQVPLRPMTY sequence was substituted by each of the 19 amino acids except for cysteine. The residues of the index peptide are listed horizontally at the top of the chart, and the letters along the sides indicate the residues replacing the index residue. The EC_{50} value of each peptide was calculated as the concentration of peptide that exhibited a half-maximal activation of TCR-transduced TG40 cells in response to 10^{-5} M index peptide defined as maximal. Amino acid substitution peptide analogs were tested for binding to HLA-B35 by using TAP-deficient RMA-S cells; and the concentration of the peptide that yielded a half maximal binding level (BL_{50}) was calculated as described earlier [22]. The TCR-pMHC interaction was determined by the EC_{50}/BL_{50} values, and >100 was defined as negative. The index residues at each position are outlined in black. This assay was repeated three to four times for each variant peptide.

three types. These results suggest that the length of the epitope peptide substantially influenced the cross-reactivity profiles of the cognate TCRs toward variant antigens.

The overlapping epitopes of different lengths presented by the same HLA-I are widely observed in HIV-1 infection: for example, HLA-B27-restricted Gag epitopes, KL8 (Gag263-270: KRWIILGL) and KK10 (Gag263-272: KRWIILGLNK) [7]; HLA-B57-restricted Gag peptides, KI8 (Gag162-169: KAFSPEVI) and KF11 (Gag162-172: KAFSPEVIPMF) [8]; HLA-B*54:01-restricted Pol epitopes, FT8 (Pol155-162: FPISPIET), FV9 (Pol155-163: FPISPIETV), FP10 (Pol155-164: FPISPIETVP), and FV11 (Pol 155-165: FPISPIETVPV) [9]. In all of these cases, each of these epitopes generated different CD8 T subsets; although only one of each overlapping epitopes can often be dominant *in vivo* [7–9]. In the HLA-B*35:01-restricted overlapping epitope case here, VY8 is a dominant epitope in the early phase of an HIV-1 infection, whereas RY11 becomes dominant in the chronic phase [21]; although the RM9-specific response *in vivo* has not been systematically analyzed yet. The pathways and mechanisms by which one of these epitopes becomes dominant over the others remain elusive. It would be interesting to determine the susceptibility of precursor peptides to proteasomes and other intracellular or ER-resident proteases such as ERAP1 [33] among these peptides in a future study. In contrast, it has been reported that the VY8/HLA-B35 complex shows more stability than the RY11/HLA-B35 complex in heat-denaturation experiments [6] and that such a difference in biochemical property between peptide-HLA complexes, rather than interaction between TCR and peptide-HLA complex is most likely associated with potent antiviral activity toward HIV-infected $CD4^+$ T lymphocytes by the VY8-specific CTLs [6,21]. It will therefore be intriguing to determine the thermostability profiles of all of these complexes between HLA-I molecule and overlapping peptides and compare their association with immunodominant hierarchy as well as with the antiviral potency of T lymphocytes recognizing these epitopes.

We previously found that the Arg to Thr and Tyr to Phe mutations at the position 1 and 11 in the RY11 sequence were associated with escape from CTL responses specific for RY11 and VY8, respectively [5]. Consistently, we showed here that RY11-specific TCRs (such as H231) failed to recognize peptides having the mutations at the position 1 and that VY8-specific TCRs (such as 139 and S1) were substantially reduced recognition toward the peptide with the mutation at the C-terminus (Fig. 4). These results suggest that the differential cross-reactivity profiles of TCRs specific for overlapping epitopes of different lengths contribute, at least in part, in forming sequence polymorphisms of naturally-arising CTL-escape viral variants at a population level.

One may raise a question how RM9-specific TCRs can recognize both RM9 and RY11 although RY11- and VY8-specific TCRs can only recognize the cognate peptides. In this regard, the crystal structure analyses of the peptide-HLA complexes show that the peptide can be bound with HLA in a C-terminally-extended way in some settings and that such complexes are recognized by the cognate TCRs [7,32]. It might be likely that a fraction of RY11 can be eventually bound with HLA-B*35:01 in a C-terminally-extended way and recognized by RM9-specific TCRs. Further structural study is needed to clarify whether a peptide can be bound with HLA with different modes: i.e., a C-terminal extended way or a central region bulged.

The TCR reconstruction system used here showed tetramer binding activity mostly consistent with the data generated by

Please cite this article in press as: Motozono C, et al., Cross-reactivity analysis of T cell receptors specific for overlapping HIV-1 Nef epitopes of different lengths, Microbes and Infection (2013), http://dx.doi.org/10.1016/j.micinf.2013.12.005

CTL clones except in the case of TG40-27. This TCR-reconstructed cell showed extremely weak or virtually no binding activity toward RY11/B35 or RM9/B35 tetramers (Fig. 3C), although CTL19-27 bound to both tetramers (Fig. 2B). TCR-tetramer binding on the T cell surface may be influenced by several factors [34] such as TCR-peptide-HLA binding activity itself [35], expression level of TCRs on the cell surface [36], membrane architecture of T cells [37], co-receptors including CD8 [35,38], and so on. Given that TG40-27 responded to peptide-pulsed cells when human CD8 was expressed on the cell surface, it is likely that antigen recognition by the TCR from CTL19-27 was CD8 dependent, as previously described in the case of other TCR specificities [35,38]. Further experiments are needed to reveal the possible difference in antiviral activity of CTLs whose antigen recognition is dependent or independent on co-receptors.

Acknowledgments

This research was supported by a grant-in-aid for scientific research from the Ministry of Education, Science, Sports, and Culture (MEXT) of Japan; by the Global COE Program (Global Education and Research Center Aiming at the Control of AIDS), MEXT, Japan; and by a grant-in-aid for AIDS research from the Ministry of Health, Labor, and Welfare of Japan.

References

[1] Rudolph MG, Stanfield RL, Wilson IA. How TCRs bind MHCs, peptides, and coreceptors. Annu Rev Immunol 2006;24:419–66.
[2] Tynan FE, Burrows SR, Buckle AM, Clements CS, Borg NA, Miles JJ, et al. T cell receptor recognition of a 'super-bulged' major histocompatibility complex class I-bound peptide. Nat Immunol 2005;6:1114–22.
[3] Ekeruche-Makinde J, Miles JJ, van den Berg HA, Skowera A, Cole DK, Dolton G, et al. Peptide length determines the outcome of TCR/peptide-MHCI engagement. Blood 2013;121:1112–23.
[4] Burrows JM, Bell MJ, Brennan R, Miles JJ, Khanna R, Burrows SR. Preferential binding of unusually long peptides to MHC class I and its influence on the selection of target peptides for T cell recognition. Mol Immunol 2008;45:1818–24.
[5] Ueno T, Motozono C, Dohki S, Mwimanzi P, Rauch S, Fackler OT, et al. CTL-mediated selective pressure influences dynamic evolution and pathogenic functions of HIV-1 Nef. J Immunol 2008;180:1107–16.
[6] Motozono C, Yanaka S, Tsumoto K, Takiguchi M, Ueno T. Impact of intrinsic cooperative thermodynamics of peptide-MHC complexes on antiviral activity of HIV-specific CTL. J Immunol 2009;182:5528–36.
[7] Tenzer S, Wee E, Burgevin A, Stewart-Jones G, Friis L, Lamberth K, et al. Antigen processing influences HIV-specific cytotoxic T lymphocyte immunodominance. Nat Immunol 2009;10:636–46.
[8] Goulder PJ, Tang Y, Pelton SI, Walker BD. HLA-B57-restricted cytotoxic T-lymphocyte activity in a single infected subject toward two optimal epitopes, one of which is entirely contained within the other. J Virol 2000;74:5291–9.
[9] Hashimoto M, Akahoshi T, Murakoshi H, Ishizuka N, Oka S, Takiguchi M. CTL recognition of HIV-1-infected cells via cross-recognition of multiple overlapping peptides from a single 11-mer Pol sequence. Eur J Immunol 2012;42:2621–31.
[10] Lucchiari-Hartz M, Lindo V, Hitziger N, Gaedicke S, Saveanu L, van Endert PM, et al. Differential proteasomal processing of hydrophobic and hydrophilic protein regions: contribution to cytotoxic T lymphocyte epitope clustering in HIV-1-Nef. Proc Natl Acad Sci U S A 2003;100:7755–60.
[11] Rehermann B, Chisari FV. Cell mediated immune response to the hepatitis C virus. Curr Top Microbiol Immunol 2000;242:299–325.
[12] Dong T, Stewart-Jones G, Chen N, Easterbrook P, Xu X, Papagno L, et al. HIV-specific cytotoxic T cells from long-term survivors select a unique T cell receptor. J Exp Med 2004;200:1547–57.
[13] Kosmrlj A, Read EL, Qi Y, Allen TM, Altfeld M, Deeks SG, et al. Effects of thymic selection of the T-cell repertoire on HLA class I-associated control of HIV infection. Nature 2010;465:350–4.
[14] Iglesias MC, Almeida JR, Fastenackels S, van Bockel DJ, Hashimoto M, Venturi V, et al. Escape from highly effective public CD8+ T-cell clonotypes by HIV. Blood 2011;118:2138–49.
[15] Chen H, Ndhlovu ZM, Liu D, Porter LC, Fang JW, Darko S, et al. TCR clonotypes modulate the protective effect of HLA class I molecules in HIV-1 infection. Nat Immunol 2012;13:691–700.
[16] Hoof I, Perez CL, Buggert M, Gustafsson RK, Nielsen M, Lund O, et al. Interdisciplinary analysis of HIV-specific CD8+ T cell responses against variant epitopes reveals restricted TCR promiscuity. J Immunol 2010;184:5383–91.
[17] Ladell K, Hashimoto M, Iglesias MC, Wilmann PG, McLaren JE, Gras S, et al. A, Molecular basis for the control of preimmune escape variants by HIV-specific CD8(+) T cells. Immunity 2013;38:425–36.
[18] Culmann-Penciolelli B, Lamhamedi-Cherradi S, Couillin I, Guegan N, Levy JP, Guillet JG, et al. Identification of multirestricted immunodominant regions recognized by cytolytic T lymphocytes in the human immunodeficiency virus type 1 Nef protein. J Virol 1994;68:7336–43.
[19] Choppin J, Cohen W, Bianco A, Briand JP, Connan F, Dalod M, et al. Characteristics of HIV-1 Nef regions containing multiple CD8+ T cell epitopes: wealth of HLA-binding motifs and sensitivity to proteasome degradation. J Immunol 2001;166:6164–9.
[20] Milicic A, Price DA, Zimbwa P, Booth BL, Brown HL, Easterbrook PJ, et al. CD8+ T cell epitope-flanking mutations disrupt proteasomal processing of HIV-1 Nef. J Immunol 2005;175:4618–26.
[21] Ueno T, Idegami Y, Motozono C, Oka S, Takiguchi M. Altering effects of antigenic variations in HIV-1 on antiviral effectiveness of HIV-specific CTLs. J Immunol 2007;178:5513–23.
[22] Ueno T, Tomiyama H, Takiguchi M. Single T cell receptor-mediated recognition of an identical HIV-derived peptide presented by multiple HLA class I molecules. J Immunol 2002;169:4961–9.
[23] Ueno T, Tomiyama H, Fujiwara M, Oka S, Takiguchi M. HLA class I-restricted recognition of an HIV-derived epitope peptide by a human T cell receptor alpha chain having a Vdelta1 variable segment. Eur J Immunol 2003;33:2910–6.
[24] Smith KJ, Reid SW, Stuart DI, McMichael AJ, Jones EY, Bell JI. An altered position of the alpha 2 helix of MHC class I is revealed by the crystal structure of HLA-B*3501. Immunity 1996;4:203–13.
[25] Gerber PR, Muller K. MAB, a generally applicable molecular force field for structure modelling in medicinal chemistry. J Comput Aided Mol Des 1995;9:251–68.
[26] Onufriev A, Bashford D, Case DA. Modification of the generalized born model suitable for macromolecules. J Phys Chem B 2000;104:3712–20.
[27] Goto J, Kataoka R, Muta H, Hirayama N. ASEDock-docking based on alpha spheres and excluded volumes. J Chem Inf Model 2008;48:583–90.
[28] Tomiyama H, Miwa K, Shiga H, Moore YI, Oka S, Iwamoto A, et al. Evidence of presentation of multiple HIV-1 cytotoxic T lymphocyte epitopes by HLA-B*3501 molecules that are associated with the accelerated progression of AIDS. J Immunol 1997;158:5026–34.
[29] Rowland-Jones S, Sutton J, Ariyoshi K, Dong T, Gotch F, McAdam S, et al. HIV-specific cytotoxic T-cells in HIV-exposed but uninfected Gambian women. Nat Med 1995;1:59–64.
[30] Rist MJ, Theodossis A, Croft NP, Neller MA, Welland A, Chen Z, et al. HLA peptide length preferences control CD8+ T cell responses. J Immunol 2013;191:561–71.
[31] Hornell TM, Martin SM, Myers NB, Connolly JM. Peptide length variants p2Ca and QL9 present distinct conformations to L(d)-specific T cells. J Immunol 2001;167:4207–14.
[32] Collins EJ, Garboczi DN, Wiley DC. Three-dimensional structure of a peptide extending from one end of a class I MHC binding site. Nature 1994;371:626–9.

Please cite this article in press as: Motozono C, et al., Cross-reactivity analysis of T cell receptors specific for overlapping HIV-1 Nef epitopes of different lengths, Microbes and Infection (2013), http://dx.doi.org/10.1016/j.micinf.2013.12.005

[33] York IA, Chang SC, Saric T, Keys JA, Favreau JM, Goldberg AL, et al. The ER aminopeptidase ERAP1 enhances or limits antigen presentation by trimming epitopes to 8-9 residues. Nat Immunol 2002;3:1177–84.

[34] Wooldridge L, Lissina A, Cole DK, van den Berg HA, Price DA, Sewell AK. Tricks with tetramers: how to get the most from multimeric peptide-MHC. Immunology 2009;126:147–64.

[35] Laugel B, van den Berg HA, Gostick E, Cole DK, Wooldridge L, Boulter J, et al. Different T cell receptor affinity thresholds and CD8 coreceptor dependence govern cytotoxic T lymphocyte activation and tetramer binding properties. J Biol Chem 2007;282:23799–810.

[36] Lissina A, Ladell K, Skowera A, Clement M, Edwards E, Seggewiss R, et al. Protein kinase inhibitors substantially improve the physical detection of T-cells with peptide-MHC tetramers. J Immunol Methods 2009;340:11–24.

[37] Drake 3rd DR, Braciale TJ. Cutting edge: lipid raft integrity affects the efficiency of MHC class I tetramer binding and cell surface TCR arrangement on CD8+ T cells. J Immunol 2001;166:7009–13.

[38] Cole DK, Laugel B, Clement M, Price DA, Wooldridge L, Sewell AK. The molecular determinants of CD8 co-receptor function. Immunology 2012;137:139–48.

Please cite this article in press as: Motozono C, et al., Cross-reactivity analysis of T cell receptors specific for overlapping HIV-1 Nef epitopes of different lengths, Microbes and Infection (2013), http://dx.doi.org/10.1016/j.micinf.2013.12.005

JVI
Journals.ASM.org

Impaired Nef Function Is Associated with Early Control of HIV-1 Viremia

Xiaomei T. Kuang,[a] Xiaoguang Li,[b] Gursev Anmole,[a] Philip Mwimanzi,[a,c] Aniqa Shahid,[c] Anh Q. Le,[c] Louise Chong,[a] Hua Qian,[b] Toshiyuki Miura,[d*] Tristan Markle,[a] Bemuluyigza Baraki,[a,c] Elizabeth Connick,[e] Eric S. Daar,[f] Heiko Jessen,[g] Anthony D. Kelleher,[h] Susan Little,[i] Martin Markowitz,[j] Florencia Pereyra,[d,k*] Eric S. Rosenberg,[k] Bruce D. Walker,[d,k,l] Takamasa Ueno,[b,m] Zabrina L. Brumme,[c,n] Mark A. Brockman[a,c,n]

Department of Molecular Biology and Biochemistry, Simon Fraser University, Burnaby, Canada[a]; Center for AIDS Research, Kumamoto University, Kumamoto, Japan[b]; Faculty of Health Sciences, Simon Fraser University, Burnaby, Canada[c]; Ragon Institute of MGH, MIT and Harvard, Cambridge, Massachusetts, USA[d]; Department of Medicine, University of Colorado—Denver, Denver, Colorado, USA[e]; David Geffen School of Medicine, University of California, Los Angeles, Los Angeles, USA[f]; Jessen-Jessen Praxis, Berlin, Germany[g]; Kirby Institute for Infection and Immunity in Society, University of New South Wales, Sydney, Australia[h]; Division of Infectious Diseases, University of California, San Diego, San Diego, USA[i]; Aaron Diamond AIDS Research Center, New York, New York, USA[j]; Division of Infectious Diseases, Massachusetts General Hospital, Boston, Massachusetts, USA[k]; Howard Hughes Medical Institute, Chevy Chase, Maryland, USA[l]; International Research Center for Medical Sciences (IRCMS), Kumamoto University, Kumamoto, Japan[m]; British Columbia Centre for Excellence in HIV/AIDS, Vancouver, Canada[n]

ABSTRACT

Host and viral factors influence the HIV-1 infection course. Reduced Nef function has been observed in HIV-1 controllers during the chronic phase, but the kinetics and mechanisms of Nef attenuation in such individuals remain unclear. We examined plasma RNA-derived Nef clones from 10 recently infected individuals who subsequently suppressed viremia to less than 2,000 RNA copies/ml within 1 year postinfection (acute controllers) and 50 recently infected individuals who did not control viremia (acute progressors). Nef clones from acute controllers displayed a lesser ability to downregulate CD4 and HLA class I from the cell surface and a reduced ability to enhance virion infectivity compared to those from acute progressors (all $P < 0.01$). HLA class I downregulation activity correlated inversely with days postinfection (Spearman's $R = -0.85$, $P = 0.004$) and positively with baseline plasma viral load (Spearman's $R = 0.81$, $P = 0.007$) in acute controllers but not in acute progressors. Nef polymorphisms associated with functional changes over time were identified in follow-up samples from six controllers. For one such individual, mutational analyses indicated that four polymorphisms selected by HLA-A*31 and B*37 acted in combination to reduce Nef steady-state protein levels and HLA class I downregulation activity. Our results demonstrate that relative control of initial HIV-1 viremia is associated with Nef clones that display reduced function, which in turn may influence the course of HIV-1 infection. Transmission of impaired Nef sequences likely contributed in part to this observation; however, accumulation of HLA-associated polymorphisms in Nef that impair function also suggests that $CD8^+$ T-cell pressures play a role in this phenomenon.

IMPORTANCE

Rare individuals can spontaneously control HIV-1 viremia in the absence of antiretroviral treatment. Understanding the host and viral factors that contribute to the controller phenotype may identify new strategies to design effective vaccines or therapeutics. The HIV-1 Nef protein enhances viral pathogenesis through multiple mechanisms. We examined the function of plasma HIV-1 RNA-derived Nef clones isolated from 10 recently infected individuals who subsequently controlled HIV viremia compared to the function of those from 50 individuals who failed to control viremia. Our results demonstrate that early Nef clones from HIV controllers displayed lower HLA class I and CD4 downregulation activity, as well as a reduced ability to enhance virion infectivity. The accumulation of HLA-associated polymorphisms in Nef during the first year postinfection was associated with impaired protein function in some controllers. This report highlights the potential for host immune responses to modulate HIV pathogenicity and disease outcome by targeting cytotoxic T lymphocyte (CTL) epitopes in Nef.

Rare HIV-1-infected individuals who suppress plasma viral loads (pVL) to fewer than 50 RNA copies/ml ("elite controllers" [EC]) or to fewer than 2,000 RNA copies/ml ("viremic controllers") in the absence of antiretroviral therapy provide an opportunity to identify host and viral determinants of spontaneous HIV-1 control that could aid development of vaccines or novel therapeutics. However, the mechanisms underlying the HIV-1 controller phenotype, particularly those acting at the acute/early infection stage, remain incompletely defined.

Host genetic and immune factors influence HIV-1 control. Protective human leukocyte antigen (HLA) class I alleles, notably B*57 and B*27, have been associated with lower pVL and delayed rates of disease progression in natural-history studies (1, 2) and genome-wide-association studies (3–5), and these alleles are enriched among HIV-1 controllers (6–8). Polyfunctional cytokine production and rapid perforin or granzyme expression are also frequently observed in $CD8^+$ cytotoxic T lymphocytes (CTL) from controllers (9–11), suggesting that qualitative immune characteristics also influence viremia (12). While CTL responses targeting the HIV-1 Gag protein are likely to be central mediators of immune control (13), responses to Nef might also be beneficial (14, 15). Taking the data together, cellular immune responses recognizing mutationally constrained viral epitopes presented by certain HLA alleles are believed to be key to effective HIV-1 suppression (16).

Viral genetic factors also influence HIV-1 pathogenesis. *In vitro* viral replication capacity independently associates with early clinical markers of pathogenesis (17). Moreover, Gag, Pol, and Nef proteins from chronically infected EC have consistently displayed relative functional attenuation (18–21), suggesting that impaired viral function is a hallmark of this phenotype (22). In many cases, host expression of protective HLA alleles or the presence of specific HLA-associated escape mutations or both are associated with even lower viral protein function in these individuals, suggesting that adaptation to host HLA-restricted CTL can further attenuate HIV-1. Consistent with the observed "genetic fragility" (i.e., mutationally sensitive nature) of the HIV-1 p24 capsid protein as a result of its critical role in virion assembly (23), functional costs of CTL escape have been observed most readily in Gag (24–28), but immune-driven functional costs have also been demonstrated in Pol (18, 29) and Env (19, 30). The observation that compensatory mutations that offset the functional impact of escape arise more frequently in progressors than in controllers (28, 31) (likely due in part to severely reduced viral replication in the latter individuals) further complicates the study of HIV-1 adaptation to its host and its pathogenic consequences.

A major gap in our knowledge of HIV-1 controllers is a poor understanding of early events following infection that contribute to clinical outcome in these individuals (22). HIV-1 controller cohorts are generally comprised of individuals identified during the chronic phase; as such, sequence/function relationships in early controller viruses and the role of early host immune responses in modulating viral pathogenesis remain incompletely defined. A recent study by our group demonstrated reduced *in vitro* replication capacities of recombinant HIV-1 strains encoding *gag* and *protease* from 18 recently infected individuals who subsequently controlled pVL to less than 2,000 RNA copies/ml compared to those from 45 individuals who progressed with higher viremia, which was likely due to both transmission of less-fit strains and selection of CTL escape mutations by protective HLA alleles (32). It remains to be determined whether other viral proteins in controllers exhibit similar early evidence of relative attenuation. In particular, we hypothesized that HIV-1 Nef, an ~27-kDa accessory protein that enhances viral pathogenesis, may play an early role in determining HIV-1 control. Nef interacts with a number of host proteins and performs multiple functions (33), including downregulation of cell surface CD4 (34) and HLA class I (35), upregulation of HLA class II invariant chain (CD74) (36), enhancement of virion infectivity (37), stimulation of viral replication in peripheral blood mononuclear cells (PBMC) (38), and alteration of T cell receptor (TCR) signaling (39, 40). Nef's relevance to pathogenesis is illustrated by the exceptionally slow disease progression exhibited by individuals infected with *nef*-deleted or *nef*-defective HIV-1 (41–44).

To enhance our understanding of early Nef function in HIV-1 controllers, we examined the sequence and *in vitro* function of plasma RNA-derived clonal *nef* sequences from 10 recently infected individuals who subsequently suppressed pVL to less than 2,000 RNA copies/ml in the absence of treatment (acute controllers; "AC") and from 50 recently infected individuals who failed to suppress viremia (acute progressors, "AP"). Nef clones were assessed for their ability to downregulate CD4 and HLA class I and to enhance virion infectivity. Longitudinal assessments were also performed on Nef clones from six AC from whom follow-up samples were available, including one individual for whom the impact of HLA-associated polymorphisms on Nef function was explored in detail using site-directed mutagenesis. Overall, our results indicate that HIV-1 viremia control is associated with the presence of early Nef clones that display reduced *in vitro* function. This reduced function is likely a result of acquisition of partially attenuated viral strains at transmission, combined with the subsequent selection of escape mutations by host CTL responses that impair one or more Nef activities.

MATERIALS AND METHODS

Study subjects. This study was approved by the Research Ethics Boards at Simon Fraser University (Burnaby, BC, Canada) and the Massachusetts General Hospital (Boston, MA). As described previously (32), participants were identified at sites in the United States, Australia, and Germany during acute/early HIV-1 infection as defined by the Acute Infection Early Disease Research Program (AIEDRP) criteria (45). Study subjects included $n = 10$ acute controllers (AC) who spontaneously suppressed HIV-1 plasma viremia to less than 2,000 RNA copies/ml during the first year of infection and $n = 50$ acute progressors (AP) who failed to suppress HIV-1 viremia to less than 2,000 RNA copies/ml during this time (Fig. 1).

Received 7 May 2014 Accepted 18 June 2014
Published ahead of print 25 June 2014
Editor: G. Silvestri
Address correspondence to Mark A. Brockman, mark_brockman@sfu.ca.
* Present address: Toshiyuki Miura, Medical Affairs Department, ViiV Healthcare K.K., Tokyo, Japan; Florencia Pereyra, Novartis Institute for Biomedical Research, Cambridge, MA, USA.
X.T.K. and X.L. contributed to this article as first authors.
T.U., Z.L.B., and M.A.B. contributed to this article as senior authors.
Supplemental material for this article may be found at http://dx.doi.org/10.1128/JVI.01334-14.

doi:10.1128/JVI.01334-14

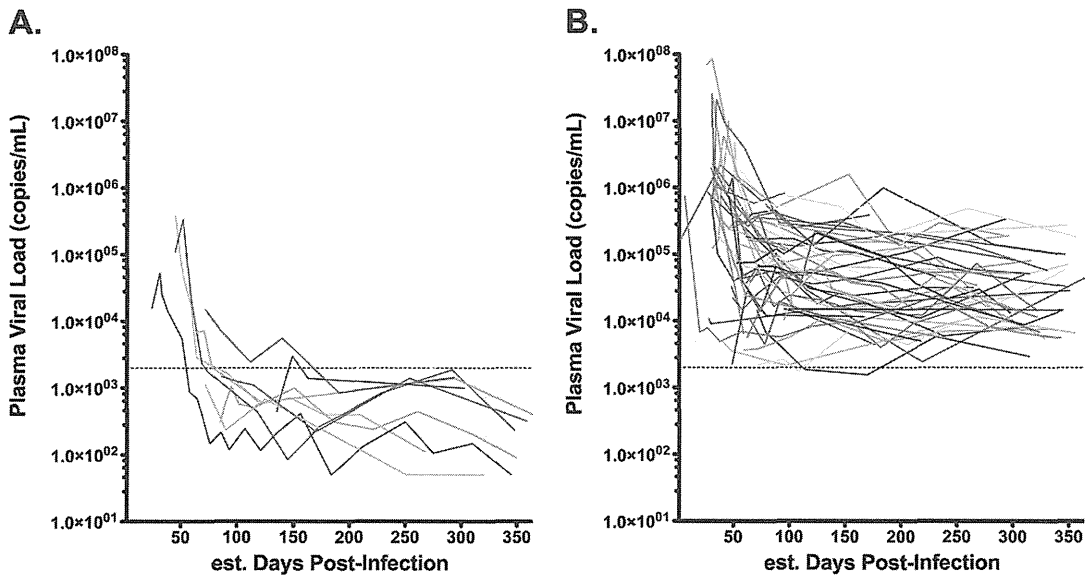

FIG 1 Plasma viral loads of AC and AP during the first year postinfection. Lines illustrate the plasma viral load (in HIV RNA copies/ml) for each participant. (A) Data are plotted for 10 AC who achieved viremic control (<2,000 RNA copies/ml) within the first year of infection. (B) Data are plotted for 50 AP who did not control viremia during this time. Dashed lines indicate the threshold value (2,000 RNA copies/ml) used to identify acute controllers.

The earliest available plasma samples were studied. For AC and AP, these were collected an estimated median of 72 (interquartile range [IQR], 57 to 99) days and 56 (IQR, 39 to 75) days postinfection, respectively (Table 1). Additional follow-up analyses were conducted for six AC for whom samples were available (Table 1). All participants remained untreated for a minimum of 1 year postinfection.

Viral (HIV-1 Nef) and Host (HLA class I) genotyping. HIV-1 *nef* gene products were amplified from plasma RNA as described previously (32). Briefly, nested reverse transcription-PCR (RT-PCR) was performed using HIV-1-specific primers, where the second-round forward and reverse primers included EcoRI and SacII restriction sites, respectively, used for cloning. Amplicons were ligated into pIRES2-enhanced green fluorescent protein (EGFP) (Clontech), transformed into *Escherichia cloni* 10G cells (Lucigen), and selected on LB agar plates containing kanamycin. Colonies were screened by restriction enzyme digest to verify *nef* insertion. Nested RT-PCR amplicons and pIRES2-*nef*-EGFP clones were sequenced bidirectionally on a 3130xl or 3730xl automated DNA sequencer (Applied Biosystems, Inc.). Chromatograms were analyzed using Sequencher v5.0 (Genecodes) or RECall (46). In bulk sequences, nucleotide mixtures were called if the subdominant peak height exceeded 25% (Sequencher) or the subdominant peak area exceeded 20% (RECall) of the dominant peak. All sequences were confirmed to be HIV-1 subtype B using the Recombinant Identification Program (RIP; http://www.hiv.lanl.gov/content/sequence/RIP/RIP.html). *nef* sequences were aligned to HXB2 using an in-house tool based on the HyPhy platform (47), and phylogenetic analysis was conducted using PhyML (48, 49). Each clone sequence was also compared to the original bulk sequence to enumerate the number of amino acid differences between them. These steps ensured that each Nef clone encoded an intact open reading frame and was free of gross genetic defects (e.g., large deletions) and that clones chosen for functional analysis were representative of each individual's circulating viral quasispecies. HLA class I typing was performed using genomic DNA extracted from PBMC or plasma using sequence-based methods (50).

CD4 and HLA class I downregulation assays. Nef-mediated CD4 and HLA class I downregulation function was assessed by flow cytometry following transient transfection, as described previously (21). Briefly, 3×10^5 CEM-A*02-positive (CEM-A*02$^+$) cells in Opti-MEM (Life Technologies) were transfected with 5 μg of pIRES2-*nef*-EGFP by electroporation (Bio-Rad Gene Pulser MXcell) (square wave, 250 V, 2,000 μF, infinite Ω, 25 ms) and recovered in R10+ medium (RPMI 1640 containing 10% fetal calf serum, 2 mM L-glutamine, 100 U of penicillin/ml, and 100 μg of streptomycin/ml) (Sigma). After 24 h, unfixed transfected cells were stained with allophycocyanin (APC)-labeled anti-CD4 and phycoerythrin (PE)-labeled anti-HLA-A*02 antibodies (BD Biosciences), and surface expression of these molecules was detected using a Guava easyCyte 8HT flow cytometer (Millipore). For each Nef clone, the median fluorescence intensity (MFI) of CD4 or HLA class I on GFP-positive (Nef-producing) cells was normalized to that of cells transfected with a positive control (pIRES2-EGFP containing SF2 strain Nef; Nef_{SF2}) and a negative control (empty pIRES2-EGFP) using the following formula: $(MFI_{patient\ Nef} - MFI_{negative\ control})/(MFI_{positive\ control} - MFI_{negative\ control})$. Normalized values less than 1.0 represent downregulation activities lower than those of the positive-control Nef_{SF2}, while values greater than 1.0 represent downregulation activities higher than those of Nef_{SF2}. The calculated value of the negative control is zero. Each clone was tested in a minimum of 3 replicates, and the results were averaged.

Virion infectivity assays. *nef* clones were transferred into a pNL4.3 backbone plasmid as described previously (51) and confirmed by sequencing. Recombinant viruses carrying *nef* from HIV-1 strain SF2 (NL4.3-nef_{SF2}) and those lacking *nef* (NL4.3Δ*nef*) served as positive and negative controls, respectively. Infectious viruses were generated by transfection of HEK-293T cells with each proviral clone, and virus-containing supernatant was harvested at 48 h, as described previously (52). Viral stocks were quantified using a $p24^{Gag}$ enzyme-linked immunosorbent assay (ELISA) (ZeptoMetrix Corp.), and aliquots were stored at −80°C until use. Recombinant virus infectivity was determined by exposing 10^4 TZM-bl cells (catalog no. 8129; NIH AIDS Reagent Program) to 3 ng $p24^{Gag}$ virus stock followed by chemiluminescence detection 48 h later, as described previously (53). Infectivity values represent the means of the results of duplicate experiments, normalized to NL4.3-nef_{SF2}, such that values less than 1.0 or greater than 1.0 indicated lower or higher activity than the positive-control strain, respectively.

Western blot analysis. Steady-state Nef protein levels were measured by Western blotting for a subset of AC and AP clones. For this, 5×10^6 CEM-A*02$^+$ cells were transfected with 10 μg of pIRES2-*nef*-EGFP using electroporation. After 24 h, cells were pelleted, lysed, and analyzed as